A Theoretical Investigation of the Triplet Carbon Atom C(^{3}P) + Vinyl Radical C$_2$H$_3$(^{2}A′) Reaction and Thermochemistry of C$_3$H$_n$ ($n = 1$−4) Species

Thanh Lam Nguyen,[†] Alexander M. Mebel,*,[†] and Ralf I. Kaiser[†,‡]

Institute of Atomic and Molecular Science, Academia Sinica, P.O. Box 23-166, Taipei 10764, Taiwan, and Department of Physics, National Taiwan University, Taipei 107, Taiwan

The mechanism for the C(^{3}P) + C$_2$H$_3$ reaction has been studied via ab initio calculations to investigate possible formations of C$_3$H$_2$ and C$_3$H isomers in an extraterrestrial environment, combustion processes, and CVD. The C(^{3}P) + C$_2$H$_3$ reaction, which produces C$_3$H$_3$ radical intermediates on the ground-state potential energy surface (PES), is studied employing the B3LYP/6-311G(d,p) and RCCSD(T)/6-311+G(3df,2p) levels of theory. Initially formed C$_3$H$_3$ intermediates have enough energy to undergo unimolecular rearrangements. Further, H or H$_2$ eliminations then lead to C$_3$H$_2$ or C$_3$H fragments. The most energetically favorable channel is found to be the formation of ground-state singlet cyclopropenylidene (*c*-C$_3$H$_2$, ^{1}A$_1$) by splitting H from cycloprop-2-enyl (*c*-C$_3$H$_3$, ^{2}A′). The other reaction mechanisms leading to H$_2$CCC(^{1}A$_1$) + H, HCCCH(^{3}B) + H, and H$_2$ + HCCC(^{2}Π) exhibit barriers only 1−5 kcal/mol higher than those to produce H + *c*-C$_3$H$_2$. Detailed RRKM calculations will be needed to predict the product branching ratios under various reaction conditions. The C(^{3}P) + C$_2$H$_3$ reaction channel, yielding intermediate C$_3$H$_3$ radicals on the first excited doublet state PES, is also studied by utilizing the CASSCF(11,11)/6-311+G(d,p) and MRCI+D(7,8)/ANO(2+) levels of theory. Three local minima and six transition states are located on the excited-state C$_3$H$_3$ PES. Various H and H$_2$ loss channels are studied as well. The C−H fission of H$_2$CCCH(1^2A″) leading to HCCCH(1^1A″) + H is the most energetically favorable channel. Finally, thermochemical parameters for the C$_3$H$_n$ ($n = 1$−4) species are determined by employing the G3 theory and the CCSD(T)/6-311+G(3df,2p) method. The differences between the calculated results and available literature data do not normally exceed 1−2 kcal/mol. On the basis of the present calculations and previous theoretical and experimental data, $\Delta H_f^o{}_{298}$(H$_2$CCCH) = 84.5 ± 1 kcal/mol, $\Delta H_f^o{}_{298}$(*c*-C$_3$H$_3$) = 114.5 ± 2 kcal/mol, $\Delta H_f^o{}_{298}$(H$_3$CCC) = 124 ± 2 kcal/mol, $\Delta H_f^o{}_{298}$(*c*-C$_3$H$_2$) = 118.0 ± 1 kcal/mol, $\Delta H_f^o{}_{298}$(H$_2$CCC) = 133 ± 1 kcal/mol, $\Delta H_f^o{}_{298}$[HCCCH(^{3}B)] = 132.5 ± 1 kcal/mol, $\Delta H_f^o{}_{298}$[HCCCH-(^{1}A$_1$)] = 144 ± 1 kcal/mol, $\Delta H_f^o{}_{298}$[HCCC(^{2}Π)] = 173 ± 2 kcal/mol, and $\Delta H_f^o{}_{298}$(*c*-C$_3$H) = 170 ± 2 kcal/mol are recommended.

1. Introduction

Singlet cyclopropenylidene (*c*-C$_3$H$_2$) is one of the most abundant molecules in the interstellar environment.[1] However, the formation mechanism of this cyclic molecule together with its H$_2$CCC isomer has not been established either experimentally or theoretically.[2] Chemical models of multiple ion−molecule reactions for the formation of *c*-C$_3$H$_2$ have been suggested.[3] These approaches, however, neither reproduced the fractional abundances (isomer ratios) of *c*-C$_3$H$_2$ vs H$_2$CCC nor accounted for high deuterium enrichment observed in *c*-C$_3$DH vs *c*-C$_3$H$_2$.[2] Hence, it was proposed that the reaction of atomic carbon C(^{3}P) with vinyl radical (C$_2$H$_3$) can replace the ion−molecule based synthesis steps to form C$_3$H$_2$ isomers through a single reactive encounter.[2]

A theoretical model for the C(^{3}P) + C$_2$H$_3$ reaction investigated in this paper is presented by the following scheme:
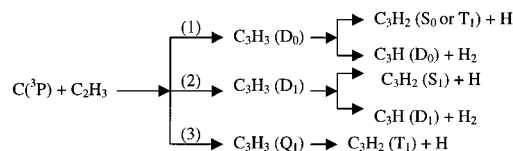
While channels 2 and 3 have not been investigated so far to our knowledge, channel 1 has been the subject of several experimental and theoretical studies. Here, C$_3$H$_3$(D$_0$) radicals are produced as highly reactive intermediates, followed by splitting atomic or molecular hydrogen to C$_3$H$_2$ or C$_3$H isomers, respectively.[4−8] The C$_3$H$_3$ radicals are also thought to be important intermediates to form the first aromatic ring by recombination of two propargyl radicals, followed by an unimolecular rearrangement.[9,10] Because of their significance, numerous experimental results and theoretical calculations have been reported concerning C$_3$H$_3$.[4−46] The equilibrium structure, vibrational frequencies, and ionization potential of the most stable C$_3$H$_3$ isomer, propargyl radical (H$_2$CCCH), were calculated by Botschwina et al.[11] at various high theoretical levels,

---
* To whom correspondence should be addressed. Fax: (+886)-2-23620200. E-mail: Mebel@po.iams.sinica.edu.tw.
  [†] Academia Sinica.
  [‡] National Taiwan University.

such as MRCI, CCSD(T), and CEPA-1. The computed results were in good agreement with experiment.[12]

Mechanism for isomerization of C$_3$H$_3$ radicals, followed by atomic or molecular hydrogen elimination to C$_3$H$_2$ or C$_3$H, was studied theoretically by Walch[4] and later by Vereecken et al.[5] The results obtained by Vereecken et al. indicate that the energetically most favorable path leads to the formation of c-C$_3$H$_2$. Vereecken et al. constructed the C$_3$H$_3$ potential energy surface (PES) employing the B3LYP/6-31G(d,p) and CASPT2 levels of theory. However, this approach may or may not provide a chemical accuracy ($\pm$ 1–2 kcal/mol). In some cases, transition states for H loss do not exist at B3LYP/6-31G(d,p). Higher theoretical levels are needed in order to refine the relative energies and to obtain more accurate PES for C$_3$H$_3$.

For excited electronic states of C$_3$H$_3$ radicals, little information is available so far. Previous calculations for the two lowest-lying excited doublet states of propargyl radical were performed by Honjou et al.,[13] using the multiconfiguration self-consistent field (MCSCF) method with the 4-31G basis set. Later, Fahr et al.[14] determined the ultraviolet absorption spectrum and cross sections of propargyl radical in the gas phase in the spectral range of 230–300 nm. They also utilized various levels of theory such as CASSCF, CASPT2, CIS, and EOM-CCSD to calculate the electronic transitions in propargyl radical. Recently, Gillbert et al.[15] reported the zero kinetic energy photoelectron spectrum of H$_2$CCCH. From the experimental results, the ionization potential for propargyl radical was derived as 8.673 eV (200 kcal/mol). However, up to now first excited electronic states for other C$_3$H$_3$ isomers and PES in the first excited state are not available either from theory or experiment.

In our previous paper,[6] C$_3$H$_3$ radicals were considered as products of primary dissociation of propyne (H$_3$CCCH) and allene (H$_2$CCCH$_2$). In the present study, we report in detail the calculational results for PES of the C(^{3}P) + C$_2$H$_3$ reaction occurring through channels 1 and 2. The relative energies for channel 1 have been improved using the restricted coupled-cluster RCCSD(T) method,[47] which is available in the Molpro program,[48] in conjunction with the 6-311+G(3df,2p) basis set. In some cases, if transition states were not found at the B3LYP/6-311G(d,p) level of theory, the QCISD/6-311G(d,p) method was used to check their existence.

The PES for channel 2, the first excited doublet state PES, was calculated using the MRCI+D(7,8)/ANO(2+) level of theory. Following route 2, the C(^{3}P) + C$_2$H$_3$ reaction yields C$_3$H$_3$(D$_1$). After eliminating atomic or molecular hydrogen, C$_3$H$_3$(D$_1$) produces C$_3$H$_2$(S$_1$) or C$_3$H(D$_1$), which can be transformed to C$_3$H$_2$(S$_0$) or C$_3$H(D$_0$) by internal conversion. Finally, thermochemical data (including ionization potentials, electron and proton affinities, C–H bond dissociation energies, and heats of formation) for C$_3$H$_3$ radicals have been also calculated using the Gaussian-3 (G3) theory[49] and the UCCSD(T)/6-311+G-(3df,2p) level of theory. Some thermochemical parameters for C$_3$H, C$_3$H$_2$, and C$_3$H$_4$ isomers have been computed as well since experimental data for the C$_3$H$_n$ (n = 1–4) species are not complete.

2. Computational Methods

For the ground electronic state, the geometry of equilibrium structures and transition states of C$_3$H$_n$ (n = 1–3) has been optimized by employing the hybrid density functional B3LYP method[50] and, in some cases, the ab initio QCISD[51] or CCSD-(T)[52] methods with the 6-311G(d,p) basis set. Vibrational frequencies, calculated at the B3LYP/6-311G(d,p) level, were used for characterization of the stationary points (number of

imaginary frequencies NIMAG = 0 and 1 for local minima and transition states, respectively) and zero-point energy (ZPE) correction. Where necessary, intrinsic reaction coordinate (IRC) calculations were utilized to confirm connections between transition states and local minima. To obtain more accurate energies on the ground-state PES, we employed the RCCSD-(T) approach[47] with the large 6-311+G(3df,2p) basis set. The RCCSD(T)/6-311+G(3df,2p)//B3LYP/6-311G(d,p) + ZPE-[B3LYP/6-311G(d,p)] calculational scheme has been shown[53] to provide accuracies of 1–2 kcal/mol for atomization energies of the G2 test set of molecules. A similar RCCSD(T)/B3LYP approach has also been demonstrated to be accurate for transition-state energies.[54]

For first excited electronic state of C$_3$H$_3$ radicals and c-C$_3$H, geometry optimization of various stationary points has been carried out using the multireference CASSCF method[55] with the 6-311+G(d,p) basis set. The active space included 11 electrons distributed on 11 orbitals (7A′ + 4A″ for C_s symmetry), CASSCF(11,11). Calculations for vibrational frequencies were carried out at the CASSCF level and, where possible, at UHF/cc-pVDZ, B3LYP/6-311G(d,p), MP2/6-311G-(d,p), and QCISD/6-311G(d,p). The energies of excited-state structures were then refined by employing internally contracted MRCI[56] calculations. The active space was reduced to 7 electrons located on 8 orbitals, MRCI(7,8). The CASSCF(11,11) wave function was taken as a reference for the MRCI(7,8) computation with the Davidson correction for quadruple excitations, MRCI+D. The basis set employed in the MRCI calculations is ANO(2+), i.e., the ANO basis set[57] (4s3p2d for C and 3s2p for H) augmented with several diffuse functions for carbon atom.[58] For first excited electronic state of C$_3$H$_2$ isomers, the relative energies on excited-state PES were evaluated by summation of the relative energies on the ground-state PES and the adiabatic excitation energies, which were taken from our previous paper.[6]

For thermochemical calculations, the G3 theory,[49] RCCSD-(T), and UCCSD(T) methods were utilized. The G3 theory, a modification of the G2 theory,[59] corrects many of the deficiencies of G2 and significantly improves thermochemical parameters. The average absolute deviation of the G3 theory from experiment for 148 calculated enthalpies of formation and 299 energies is lower than that of the G2 theory.[49] RCCSD(T) and UCCSD(T) methods in conjunction with the large 6-311+G-(3df,2p) basis set were also used to compute total energies based on optimized geometries at the B3LYP/6-311G(d,p) level of theory. The B3LYP geometries and frequencies were utilized to predict ZPE and thermal corrections for thermochemichal properties.[53,54,60,61] The use of ab initio CCSD(T)/6-311+G-(3df,2p)//B3LYP/6-311G(d,p) + TC[B3LYP/6-311G(d,p)] model in combination with isodesmic approach allows us to reliably predict thermochemical properties for the C$_3$H$_n$ (n = 1–4) species with chemical accuracies of 1–2 kcal/mol. The computed values were compared with available experimental data.

The Molpro 98[48] and Gaussian 98[62] programs were employed for the calculations.

3. Results

For the ground-state PES, Table 1 presents total, zero-point, and relative energies for various C$_3$H$_n$ (n = 1–3) species calculated at the B3LYP/6-311G(d,p) and RCCSD(T)/6-311+G-(3df,2p) levels of theory. Unscaled vibrational frequencies obtained at the B3LYP/6-311G(d,p) level are collected in Table 2. Optimized geometries for local minima and transition states, computed at different levels of theory, are shown in Figures 1

TABLE 1: Calculated Total Energy, ZPE, and Relative Energy of Various C3H3 Species

	total energy (hartrees)[a]			relative energy (kcal/mol)[d]	
species	B3LYP/ 6-311G(d,p)	RCCSD(T)/ 6-311+G(3df,2p)	ZPE (kcal/mol)[c]	B3LYP/ 6-311G(d,p)	RCCSD(T)/ 6-311+G(3df,2p)
R1(C_s-^{2}A′) + C(^{3}P)	−115.78302	−115.52738	22.81	0.0	0.0
P1a(C_{2v}-^{1}A$_1$) + H(^{2}S)	−115.85182	−115.59057	17.54	−48.5	−44.9
P1b(C_2-^{3}B) + H(^{2}S)	−115.87369	−115.60768	16.22	−63.5	−57.0
P1c(C_s-^{1}A′) + H(^{2}S)	−115.85088	−115.59123	17.40	−48.0	−45.5
P2a(C_{2v}-^{1}A$_1$) + H(^{2}S)	−115.88563	−115.63386	20.14	−67.1	−69.5
P2b(C_1-^{3}A) + H(^{2}S)	−115.80543	−115.54783	18.63	−18.3	−17.0
P3(C_{2v}-^{3}B$_1$) + H(^{2}S)	−115.77439	−115.52203	19.47	2.0	0.0
P4a(C_{2v}-^{1}A$_1$) + H(^{2}S)	−115.86676	−115.61114	19.38	−56.0	−56.0
P4b(C_s-^{3}A″) + H(^{2}S)	−115.82111	−115.55186	17.91	−28.8	−20.3
P5(C_s-^{3}A″) + H(^{2}S)	−115.77662	−115.51517	17.11	−1.7	1.9
P6a(C_s-^{2}A′) + H$_2$	−115.88813	−115.62631	16.97	−71.8	−67.9
P7(C_{2v}-^{2}B$_2$) + H$_2$	−115.88835	−115.63092	18.31	−70.6	−69.5
1(C_{2v}-^{2}B$_1$)	−116.03736	−115.77402	25.69	−156.8	−151.9
2(C_s-^{2}A′)	−115.98381	−115.72546	26.55	−123.3	−120.6
3(C_{3v}-^{2}A$_1$)	−115.96585	−115.71178	26.73	−110.8	−111.8
4(C_s-^{2}A′)	−115.96909	−115.71208	26.96	−112.6	−111.8
5(C_s-^{2}A″)	−115.95964	−115.69764	24.67	−109.0	−105.0
6(C_1-^{2}A)	−115.91337	−115.64934	23.74	−80.9	−75.6
TS1/5(C_s-^{2}A″)	−115.95964	−115.69768	24.39	−109.3	−105.3
TS3/5(C_s-^{2}A′)	−115.90866	−115.64743	22.75	−78.9	−75.4
TS4/5(a)(C_1-^{2}A)	−115.95058	−115.69102	25.40	−102.6	−100.1
TS1/6(C_1-^{2}A)	−115.89632	−115.62995	22.05	−71.9	−65.1
TS3/4(C_s-^{2}A′)	−115.88675	−115.63066	24.08	−63.9	−63.6
TS1/4(C_s-^{2}A′)	−115.95268	−115.69355	24.83	−104.5	−102.3
TS2/4(C_1-^{2}A)	−115.88213	−115.62488	22.68	−62.4	−61.3
TS2/5(C_1-^{2}A)	−115.92269	−115.66535	23.86	−86.6	−85.5
TS2/6(C_1-^{2}A)	−115.89683	−115.62518	23.11	−71.2	−61.1
TS4/4(C_1∼C_2-^{2}A)	−115.88458	−115.62699	23.07	−63.5	−62.3
TS4/5(b)(C_1-^{2}A)	−115.89957	−115.64295	23.72	−72.3	−71.6
TS1-H$_2$ loss (C_s-^{2}A″)	−115.88054	−115.61400	19.45	−64.6	−57.7
TS2-H$_2$ loss (C_1-^{2}A)	−115.86004	−115.58965	20.45	−50.7	−41.5
TS1-H loss (C_s-^{2}A′)		−115.63381[b]	20.70[b]		−69.4[e]
TS2-H loss (C_s-^{2}A′)		−115.60411[b]	20.65[b]		−50.8[e]
TS3-H loss (C_1-^{2}A)		−115.61794[b]	21.31[b]		−58.8[e]
TS4-H loss (C_{2v}-^{2}A$_1$)		−115.58309[b]	19.52[b]		−38.7[e]

[a] Using geometry optimized at the B3LYP/6-311G(d,p) level, unless otherwise noted. [b] Geometry and unscaled ZPE obtained at the QCISD/6-311G(d,p) level. [c] Unscaled ZPE at the B3LYP/6-311G(d,p) level. [d] Including unscaled ZPE at the B3LYP/6-311G(d,p) level, unless otherwise noted. [e] Including ZPE scaled by 0.9776 (ref 63) at the QCISD/6-311G(d,p) level.

and 2, respectively. A profile of the ground-state PES for the C(^{3}P) + C$_2$H$_3$ reaction constructed utilizing the RCCSD(T)/6-311+G(3df,2p)//B3LYP/6-311G(d,p) approach is depicted in Figure 3.

For the first excited doublet state PES, Table 3 shows relative energies computed at the CASSCF(11,11)/6-311+G(d,p), CASSCF(11,11)/ANO(2+), MRCI(7,8)/ANO(2+), and MRCI+D-(7,8)/ANO(2+) levels of theory with geometries optimized at CASSCF(11,11)/6-311+G(d,p). Figures 4 and 5 contain optimized geometries of local minima and transition states for the C$_3$H$_3$ and c-C$_3$H radicals. The first excited-state geometries for C$_3$H$_2$ isomers are not presented here but can be found in our previous paper.[6] A profile of the first excited doublet state PES for the C(^{3}P) + C$_2$H$_3$ reaction built employing the MRCI+D-(7,8)/ANO(2+)//CASSCF(11,11)/6-311+G(d,p) approach is shown in Figure 6.

For the quartet electronic state, some stationary points are also presented in Figure 6 using relative energies calculated at the B3LYP/6-311G(d,p) level of theory. More detailed investigation of the quartet state PES is beyond the scope of this paper.

For thermochemical computations, total energies, $H_{298} - H_0$, thermal corrections of various species, calculated at the G3, RCCSD(T)/6-311+G(3df,2p), and UCCSD(T)/6-311+G(3df,2p) levels of theory, and heats of formation for different reference species are listed in Table 4. Tables 5 and 6 show thermo-

chemical parameters for C$_3$H$_3$ radicals. Table 7 presents heats of formation for charged C$_3$H$_3$ species. Thermochemical parameters for C$_3$H$_4$ isomers are collected in Table 8. Heats of formation for C$_3$H$_n$ ($n = 1-2$) are compiled in Table 9.

4. Discussion

4.1. Ground-State PES. *4.1.1. Isomerization of C$_3$H$_3$.* The addition of C(^{3}P) to C$_2$H$_3$ can occur either to the carbon atom with an unpaired electron giving isomer **5**, 2-propen-1-yl-3-ylidene, or to the C=C bond producing isomer **4**, cycloprop-1-enyl. These isomers can rearrange to other structures such as **1** (2-propynyl or propargyl), **2** (cycloprop-2-enyl), **3** (1-propynyl), and **6** (1-propen-1-yl-3-ylidene). **5** lies 46.9 kcal/mol higher in energy than the most stable isomer **1**. This value is in good agreement with that of 47.2 kcal/mol computed at the B3LYP/6-31G(d,p) level by Vereecken et al.[5] **5** can undergo four different isomerization processes. First, isomerization of **5** → **1** occurs by a 1,2-H shift. The corresponding transition state **TS1/5** with relative energy of 46.6 kcal/mol with respect to **1** has C_s symmerty and ^{2}A″ electronic state. The geometries of this transition state and **5** are similar. Due to a higher zero-point energy, **TS1/5** sits 0.3 kcal/mol below **5** indicating that **5** is very unstable and is expected to immediately rearrange to more stable isomer **1**. A similar result was also obtained by Vereecken et al. Second, the transformation of **5** → **2** occurs by concerted 1,3-H shift and ring closure. The transition state for this process

TABLE 2: Vibrational Frequencies of Various Species, Calculated at the B3LYP/6-311G(d,p) Level

species	frequencies (cm^{-1})
1(C_{2v}-^{2}B$_1$)	352 b$_2$, 403 b$_1$, 469 b$_1$, 638 b$_2$, 683 b$_1$, 1032 b$_2$, 1090 a$_1$, 1456 a$_1$, 2011 a$_1$, 3138 a$_1$, 3228 b$_2$, 3467 a$_1$
2(C_s-^{2}A′)	614 a′, 694 a″, 885 a″, 915 a′, 978 a″, 985 a′, 1032 a″, 1236 a′, 1663 a′, 3047 a′, 3238 a″, 3284 a″
3(C_{3v}-^{2}A$_1$)	306i e, 306i e, 944 a$_1$, 964 e, 964 e, 1412 a$_1$, 1472 e, 1472 e, 2251 a$_1$, 3031 a$_1$, 3093 e, 3093 e
4(C_s-^{2}A′)	638 a″, 646 a′, 767 a″, 880 a′, 1005 a′, 1041 a′, 1079 a″, 1507 a′, 1766 a′, 3060 a′, 3141 a″, 3332 a′
5(C_s-^{2}A″)	91 a′, 445 a″, 675 a″, 705 a″, 807 a′, 1041 a″, 1148 a′, 1473 a′, 1581 a′, 2850 a′, 3168 a′, 3272 a′
6(C_1-^{2}A)	136, 361, 490, 719, 772, 931, 1154, 1212, 1417, 2952, 3228, 3235
R1(C_s-^{2}A′)	713 a′, 820 a″, 922 a″, 1047 a′, 1392 a′, 1652 a′, 3039 a′, 3133 a′, 3236 a′
P1a(C_{2v}-^{1}A$_1$)	223 b$_2$, 316 b$_1$, 462 a$_1$, 794 a$_1$, 970 a$_2$, 1232 a$_1$, 1817 b$_2$, 3225 a$_1$, 3230 b$_2$
P1b(C_2-^{3}B)	105 a, 168 b, 373 a, 417 b, 423 a, 1282 a, 1714 b, 3429 b, 3438 a
P1c(C_s-^{1}A′)	CCSD(T): 301 a″, 302 a′, 425 a′, 835 a′, 974 a′, 1088 a′, 1937 a′, 3022 a′, 3438 a′
P2a(C_{2v}-^{1}A$_1$)	799 b$_1$, 892 a$_1$, 893 b$_2$, 1004 a$_2$, 1070 b$_2$, 1311 a$_1$, 1646 a$_1$, 3220 b$_2$, 3256 a$_1$
P2b(C_1-^{3}A)	565, 638, 851, 898, 921, 1084, 1668, 3087, 3321
P3(C_{2v}-^{3}B$_1$)	605 a$_2$, 651 b$_2$, 913 a$_1$, 978 b$_1$, 1029 b$_1$, 1500 a$_1$, 1744 a$_1$, 3062 a$_1$, 3140 b$_1$
P4a(C_{2v}-^{1}A$_1$)	232 b$_1$, 293 b$_2$, 1043 b$_1$, 1052 b$_2$, 1147 a$_1$, 1486 a$_1$, 2044 a$_1$, 3090 a$_1$, 3166 b$_2$
P4b(C_s-^{3}A″)	365 a′, 445 a″, 646 a″, 943 a′, 988 a′, 1355 a′, 1440 a′, 3128 a′, 3217 a′
P5(C_s-^{3}A″)	234 a′, 374 a″, 692 a″, 747 a′, 1050 a′, 1220 a′, 1319 a′, 3070 a′, 3263 a′
P6a(C_s-^{2}A′)	235 a′, 354 a′, 397 a′, 1198 a′, 1888 a′, 3374 a′
P6b($C_{\infty v}$-^{2}Π)	218i, 242, 377, 829, 1171, 1902, 3446
P7(C_{2v}-^{2}B$_2$)	540 b$_2$, 872 b$_1$, 916 b$_2$, 1222 a$_1$, 1614 a$_1$, 3222 a$_1$
TS1/5(C_s-^{2}A″)	88i a′, 434 a″, 667 a″, 687 a′, 781 a′, 1037 a′, 1141 a′, 1470 a′, 1610a′, 2793 a′, 3168 a′, 3273 a′
TS3/5(C_s-^{2}A′)	1346i a′, 227 a″, 318 a′, 488 a″, 811 a′, 1016 a′, 1035 a″, 1449 a′, 1859 a′, 2379 a′, 3114 a′, 3219 a″
TS4/5(a)(C_1-^{2}A)	378i, 662, 699, 799, 893, 1024, 1135, 1440, 1578, 3096, 3208, 3232
TS1/6(C_1-^{2}A)	637i, 316, 491, 512, 596, 831, 998, 1069, 1666, 2594, 3009, 3339
TS3/4(C_s-^{2}A′)	1234i a′, 569 a″, 685 a′, 1013 a″, 1047 a″, 1068 a′, 1187 a′, 1469 a′, 1633 a′, 1941 a′, 3067 a′, 3163 a″
TS1/4(C_s-^{2}A′)	634i a′, 317 a″, 516 a′, 576 a″, 842 a′, 974 a″, 1090 a′, 1420 a′, 1802 a′, 3150 a′, 3271 a″, 3410 a′
TS2/4(C_1-^{2}A)	1358i, 596, 701, 774, 875, 972, 1151, 1185, 1394, 1826, 3184, 3211
TS2/5(C_1-^{2}A)	906i, 648, 706, 856, 899, 1029, 1048, 1271, 1511, 2354, 3089, 3281
TS2/6(C_1-^{2}A)	870i, 242, 576, 671, 771, 838, 1026, 1205, 1586, 2919, 3066, 3266
TS4/4(C_1-^{2}A)	1087i, 375, 695, 784, 843, 991, 1125, 1419, 1552, 2014, 3167, 3172
TS4/5(b)(C_1-^{2}A)	725i, 321, 679, 859, 874, 999, 1170, 1456, 1542, 2284, 3149, 3257
TS1-H$_2$(C_s-^{2}A″)	559i, 294, 318, 379, 459, 564, 723, 1060, 1293, 1922, 3139, 3458
TS2−H$_2$(C_1-^{2}A)	1114i, 225, 323, 562, 634, 851, 904, 1168, 1334, 1932, 3094, 3275
TS1-H(C_s-^{2}A′)	QCISD: 329i a′, 91 a″, 142 a′, 791 a′, 912 a′, 917 a′, 993 a″, 1096 a″, 1311 a′, 1646 a′, 3272 a″, 3310 a′
TS2-H(C_s-^{2}A′)	QCISD: 859i a′, 176 a″, 348 a″, 387 a′, 528 a′, 1034 a″, 1053 a′, 1124 a′, 1501 a′, 1908 a′, 3146 a′, 3239 a′
TS3-H(C_1-^{2}A)	QCISD: 1086i, 269, 524, 819, 849, 923, 1043, 1078, 1294, 1556, 3256, 3295
	B3LYP: 784i, 180, 453, 819, 835, 902, 1007, 1054, 1293, 1578, 3212, 3247
TS4-H(C_{2v}-^{2}A$_1$)	QCISD: 987i a$_1$, 319 b$_1$, 438 b$_2$, 449 b$_1$, 513 a$_1$, 674 b$_2$, 907 a$_1$, 951 a$_2$, 1172 a$_1$, 1787 b$_2$, 3218 a$_1$, 3224 b$_2$

is **TS2/5** with relative energy of 66.4 kcal/mol as compared to **1**. The barriers for the forward and reverse reactions are 19.5 and 35.1 kcal/mol, respectively. Third, **5** can rearrange to **3** by a 1,2-H shift via **TS3/5**. The **TS3/5** corresponds to the highest barrier (29.6 kcal/mol) for isomerization of **5**, and the barrier for the reverse reaction is 36.4 kcal/mol. Finally, **5** → **4** rearrangement occurs via either **TS4/5a** by ring closure or **TS4/5b** by a simultaneous 1,2-H shift and ring closure. The barrier height at **TS4/5a** is 4.9 kcal/mol, 28.5 kcal/mol lower that at **TS4/5b**.

The energy for isomer **4** is 40.1 kcal/mol above **1**, 1.9 kcal/mol lower than the value of 42 kcal/mol obtained by Vereecken et al.[5] There exist four pathways for isomerization of **4** → **1**, →**2**, →**3**, and →**5**. The rearrangement of **4** → **1** occurs by ring opening. The transition state for this process, **TS1/4**, has C_s symmetry and ^{2}A′ electronic state. Since the H$_2$C−CH bond is 0.12 Å longer than the H$_2$C−C bond in **4**, opening the cycle at the H$_2$C−CH bond is more favorable than at the H$_2$C−C bond. Consequently, the barrier height (9.5 kcal/mol) for the **4** → **1** reaction is 2.2 kcal/mol lower that for the **4** → **5** reaction. The barrier for the reverse reaction, ring closure from **1** → **4**, is 49.6 kcal/mol. The transformation of **4** → **2** takes place by a 1,2-H migration. The corresponding transition state, **TS2/4**, lies 50.5 and 59.3 kcal/mol higher than the reactant and product, respectively. The value of 50.5 kcal/mol is the highest barrier for unimolecular rearrangements of **4**. The **4** → **3** reaction occurs via **TS3/4** by simultaneous 1,2-H migration and ring opening. Since the isomers are isoergic, the barrier heights in the forward and reverse directions coincide, 48.2 kcal/mol. Isomer **3** (C_{3v}-^{2}A$_1$), has two imaginary frequencies at B3LYP/6-311G(d,p). The

results, calculated by Vereecken et al.[5] using B3LYP/6-31G-(d,p), give no imaginary frequency at a C_s geometry of symmetry. We discussed earlier[6] that at the MP2/6-311G(d,p) level of theory, the ^{2}A$_1$ state has no imaginary frequency for the C_{3v} geometry and at CCSD(T)/6-311+G(3df,2p) the C_{3v} structure is 1.8 kcal/mol lower in energy than the C_s one.[6] The relative energy of **3** is the same as that of **4**, 40.1 kcal/mol with respect to **1**, and is 1.3 kcal/mol lower than the value of 43.3 kcal/mol obtained by Vereecken et al.

1 is the most stable isomer. There are three isomerization channels from **1** leading to **4**, **5**, and **6**. While the **1** → **4** and **1** → **5** paths have been described above, the **1** → **6** pathway passes through **TS1/6** and involves a 1,2-H migration. The values of 86.8 and 10.5 kcal/mol are calculated for the barrier heights for the forward and reverse reactions, respectively. The second stable isomer, **2**, is 31.3 kcal/mol above **1** in energy, which is 1.1 kcal/mol lower than the energy computed by Vereecken et al. There are also three paths from **2**, to **4**, **5**, and **6**. The latter, **2** → **6**, involves a ring opening. The transition state for this path is **TS2/6** with a barrier height of 59.5 and 14.5 kcal/mol with respect to the reactant and product, respectively. The least stable isomer, **6**, lies 76.3 kcal/mol higher in energy compared to **1**, which is 1.6 kcal/mol above the value computed in the previous study, 74.7 kcal/mol.

In general, the relative energies of isomers calculated at the B3LYP/6-31G(d,p) level by Vereecken et al.[5] agree with the present higher level results within 1−2 kcal/mol. However, differences for transition-state energies are more significant (1−5 kcal/mol) and the largest discrepancy of 5 kcal/mol is found for **TS2/6**. Similar deviations between the CCSD(T) and B3LYP
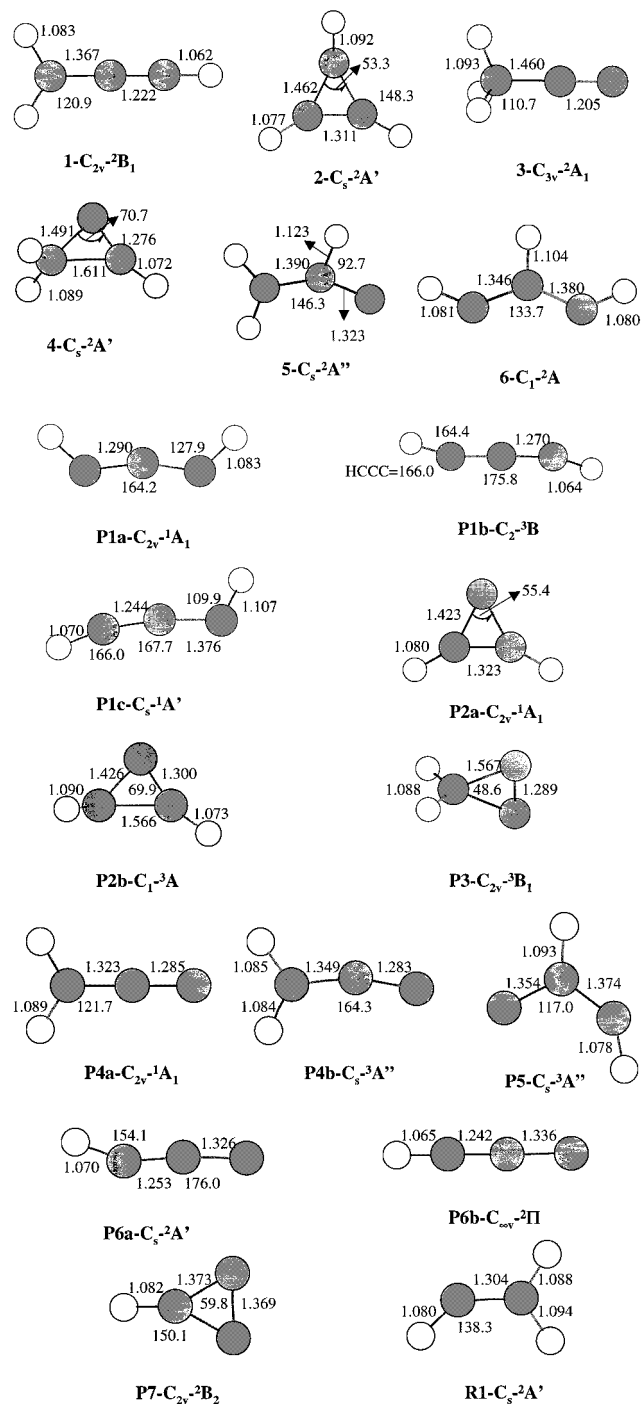
Figure 1. B3LYP/6-311G(d,p) optimized geometry of the local minima of C_3H_n ($n = 1-3$) species on the ground-state PES. Bond lengths are in Å and bond angles are in degrees. Symmetry of the species and their electronic states are also specified.

energies of transition states were found and discussed earlier for the $C_2H_3 + H_2$ reaction.[54c]

4.1.2. Atomic Hydrogen Loss in C_3H_3. Splitting atomic hydrogen from C_3H_3 radicals can yield C_3H_2 species in singlet and triplet states. The most stable isomer of C_3H_2 is c-C_3H_2, singlet cyclopropenylidene, one of the most abundant molecules in the interstellar environment.[1] The H loss process in C_3H_3 can occur with or without an exit barrier. While only the **TS3-H** exists at the B3LYP/6-31G(d,p) level,[5] we found four transition states (**TS1-H**, **TS2-H**, **TS3-H**, and **TS4-H**) employing the QCISD/6-311G(d,p) method. **TS1-H**, transition state for the **2** → c-$C_3H_2 + H$ reaction, has the same C_s symmetry and $^2A'$
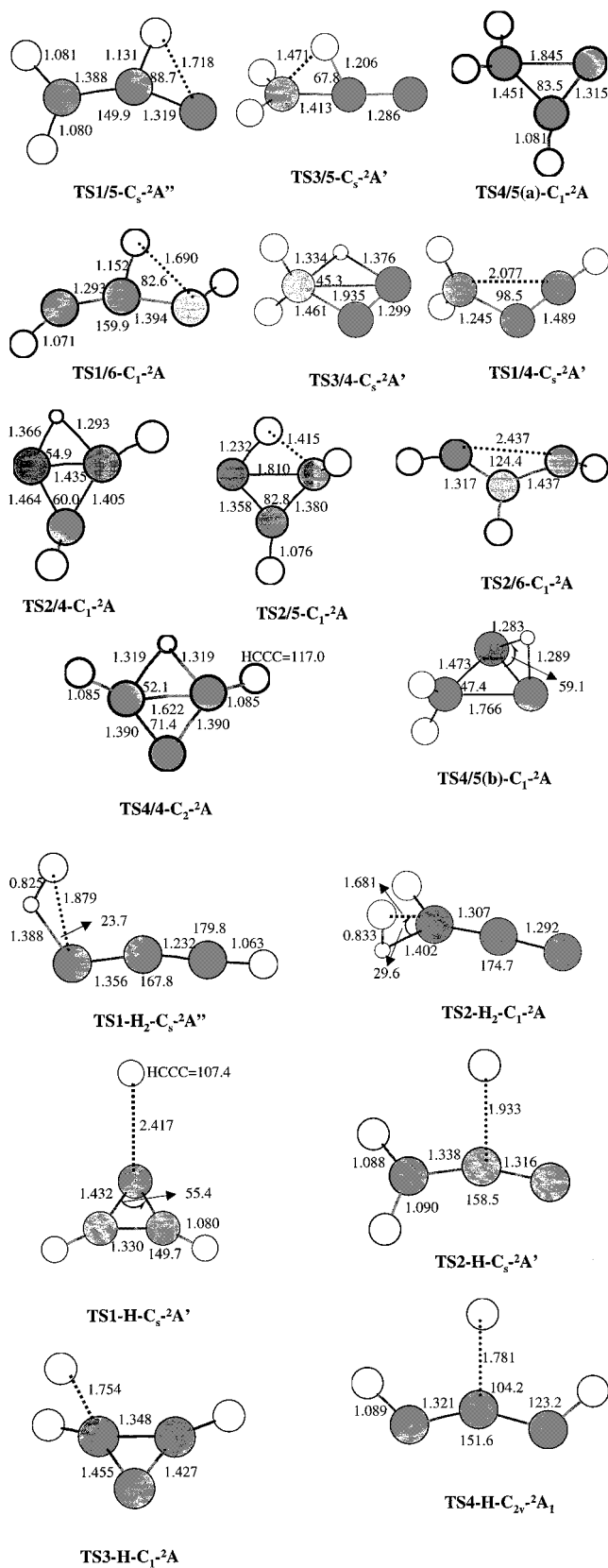
Figure 2. B3LYP/6-311G(d,p) optimized geometry of the transition states of the C(^{3}P) + C$_2$H$_3$ reaction on the ground-state PES. Bond lengths are in Å and bond angles are in degrees. Symmetry of the species and their electronic states are also specified.

electronic state as the reactant. The C−H breaking bond distance is 2.417 Å and about 0.3−0.6 Å longer than those in the other transition states. The structure of the C_3H_2 group in the **TS1-H** is similar to that of c-C_3H_2 molecule. Thus, the transition state

Figure 3. Potential energy diagram for the C(^{3}P) + C$_2$H$_3$ reaction in the ground state. The relative energies are calculated at the RCCSD(T)/6-311+G(3df,2p)//B3LYP/6-311G(d,p) + ZPE[B3LYP/6-311G(d,p)] level of theory.

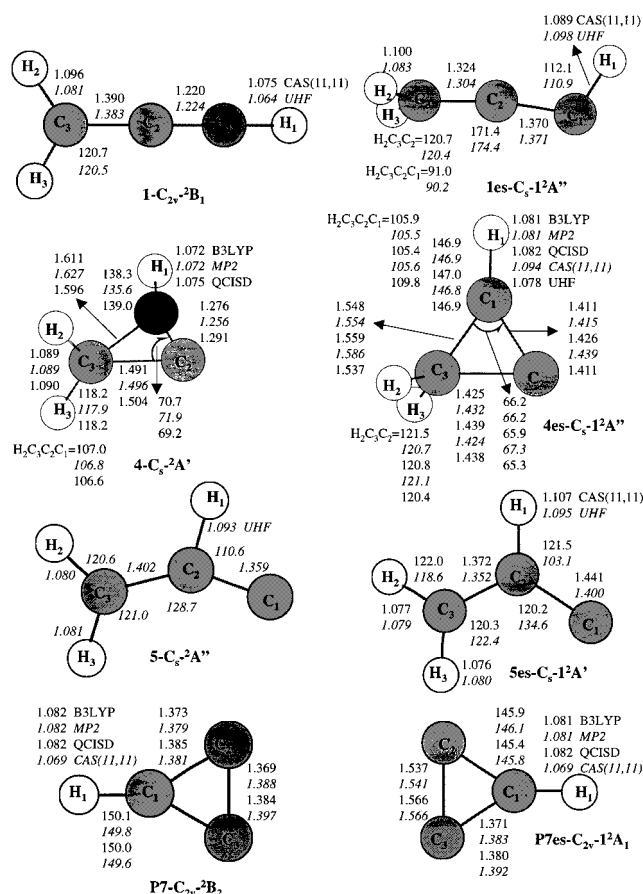**TABLE 3: Relative Energy of Various C$_3$H$_3$ Species in the First Excited Electronic State, Calculated at the CASSCF(11,11)/6-311+G(d,p), CASSCF(11,11)/ANO(2+), MRCI(7,8)/ANO(2+), and MRCI+D(7,8)/ANO(2+) Levels**

species	CASSCF(11,11)/6-311+G(d,p) (kcal/mol)	CASSCF(11,11)/ANO(2+) (kcal/mol)	MRCI(7,8)/ANO(2+) (kcal/mol)	MRCI+D(7,8)/ANO(2+) (kcal/mol)	ZPE (NIMAG) (kcal/mol)
1(C_{2v}-1^{2}B$_1$)[a]	−151.9	−151.9	−151.9	−151.9	25.69[e] (0)
1es(C_s-1^{2}A″)	−94.9	−92.3	−93.5	−94.8	27.11[h] (0)
4es(C_s-1^{2}A″)	−73.7	−74.1	−81.1	−82.9	27.10[h], 25.65[e] (0)
5es(C_s-1^{2}A′)	−93.3	−93.9	−95.5	−95.7	27.05[h] (0)
P1es(C_s-1^{2}A″)				−33.5[b]	(0)
P2aes(C_{2v}-1^{1}A$_2$)				−11.8[b]	(0)
P4es(C_{2v}-1^{1}A$_2$)				−15.4[b]	(0)
P6es($C_{\infty v}$-1^{2}Π)				−66.9[c]	(0)
P7es(C_{2v}-1^{2}A$_1$)				−46.3[d]	14.65[e], 10.79[f], 14.10[g] (0)
TS(1es/4es)(C_s-1^{2}A″)	−27.0	−27.6	−25.0	−26.4	26.45[h] (1)
TS(1es/5es)a(C_1-2^{2}A)			−29.0	−30.8	
TS(1es/5es)b(C_1-2^{2}A)			−41.7	−46.3	24.22[i] (1)
TS(4es/5es)(C_1-2^{2}A)			−69.7	−69.8	26.53[i] (1)
TS(4es/4es)(C_1-2^{2}A)			−38.3	−42.5	
TS(P1es/P6es)(C_1-2^{2}A)			−32.3	−34.0	17.38[i] (1)

[a] The total energy is −115.39816, −115.41064, −115.69475, and −115.73524 hartrees at CASSCF(11,11)/6-311+G(d,p), CASSCF(11,11)/ANO(2+), MRCI(7,8)/ANO(2+), and MRCI+D(7,8)/ANO(2+), respectively. [b] Relative energy is computed as a sum of the relative energy in the ground electronic state and the adiabatic excitation energy from ref 6. [c] From Table 1. [d] Adiabatic excitation energy computed at the UCCSD(T)/6-311+G(3df,2p)//UQCISD/6-311G(d,p) level + ZPE(UQCISD/6-311G(d,p)) is 23.2 kcal/mol. [e] At the B3LYP/6-311G(d,p) level. [f] At the MP2/6-311G(d,p) level. [g] At the QCISD/6-311G(d,p) level. [h] At the UHF/cc-pVDZ level. [i] At the s/a CAS(11,11)/6-311+G(d,p) level.

is very late, product-like. Consequently, it lies only 0.1 kcal/mol higher in energy than the products, c-C$_3$H$_2$ + H. Vereecken et al.[5] scanned the PES along the breaking C−H bond and found no barrier. The enthalpy for this reaction at 0 K is 51.1 kcal/mol, 4.2 kcal/mol below that obtained in ref 5. The value computed at 298 K, 54.9 kcal/mol (see Table 6), agrees well with the reliable CBS-QCI/APNO result (53.7 kcal/mol) of Montgomery et al.[16]

The transition state for the **5** → H$_2$CCC + H pathway is **TS2-H**, with C$_s$ symmetry and ^{2}A′ electronic state. The barrier for forward and reverse paths is 54.2 and 5.2 kcal/mol, respectively. The heat of reaction is 49.0 kcal/mol. The transition state of the **4** → c-C$_3$H$_2$ + H route, **TS3-H**, has no symmetry and gives the same product as the **2** → c-C$_3$H$_2$ + H reaction. The barrier for the H elimination is 53.0 kcal/mol, while that for the H addition is 10.7 kcal/mol, 10.6 kcal/mol higher than the barrier

Figure 4. CASSCF(11,11)/6-311+G(d,p) optimized geometry of the local minima of C_3H_3 and c-C_3H species on the first excited-state PES. Bond lengths are in Å and bond angles are in degrees. Symmetry of the species and their electronic states are also specified.

for the c-C_3H_2 + H → **2** pathway. The enthalpy of the **4** → c-C_3H_2 + H reaction is 42.3 kcal/mol. **TS4-H** is a transition state for the **6** → HCCCH(^{3}B) + H channel. It has C_{2v} symmetry, $^2A_1$ electronic state, and the highest energy (113.2 kcal/mol) relative to **1**.

We could not find transition states of H elimination from isomers **1** and **3** at both the B3LYP and QCISD levels. The saddle point search results in dissociation of hydrogen atom. Most likely, these transition states do not exist, and the addition of H to C_3H_2 species, producing **1** and **3**, has no barrier.

4.1.3. Molecular Hydrogen Loss in C_3H_3. We could only find two transition states for molecular hydrogen elimination, **TS1-H₂** and **TS2-H₂**, from isomers **1** and **3**, respectively. H₂ splitting from **1** and **3** leads to the same products, HCCC + H₂. **TS1-H₂** has C_s symmetry and $^2A''$ electronic state. The barrier height is 94.2 and 10.2 kcal/mol with respect to the reactant and products, respectively. The calculated heat of the reaction at the RCCSD-(T)/6-311+G(3df,2p) level is 84.0 kcal/mol; however, a value of 88.4 kcal/mol can be derived from the heats of formation of 84.3 and 172.7 kcal/mol for **1** (H₂CCCH) and HCCC, respectively (see Tables 5 and 9). **TS2-H₂**, for the **3** → HCCC + H₂ reaction has no symmetry. The enthalpy of this reaction is 43.9 kcal/mol at RCCSD(T)/6-311+G(3df,2p); however, another value of 48.9 kcal/mol is computed from the heats of formation for the reactant and product (see Tables 5 and 9). While the barrier for the H₂ elimination is 60.3 kcal/mol, that for the addition channel is 26.4 kcal/mol, 16.2 kcal/mol above the barrier at **TS1-H₂**. Thus, the addition of H₂ to C of HCCC, which has a C–H bond, is not energetically favorable. The more
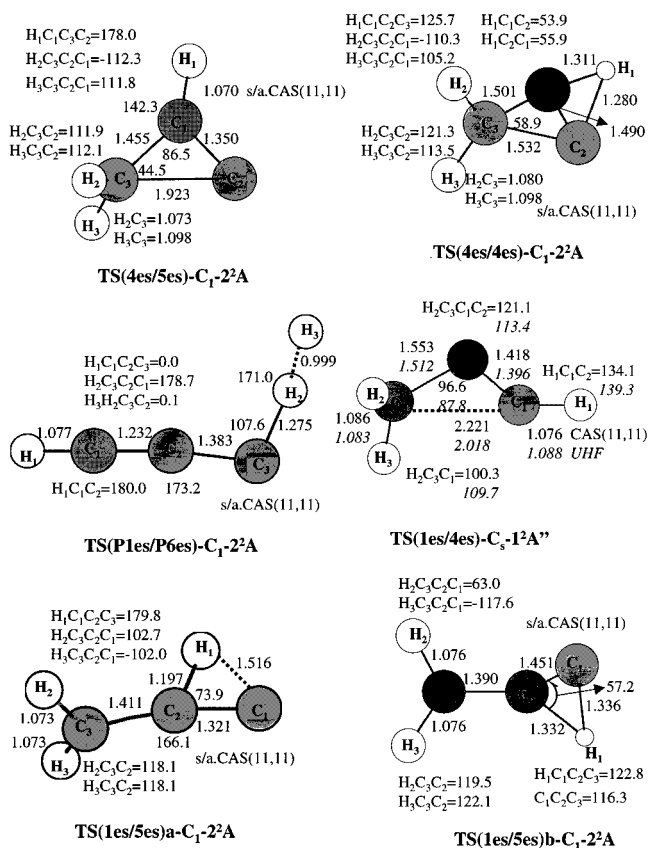
favorable reaction is the addition of H₂ to C at the opposite end of HCCC.

4.1.4. Multistep Mechanism of the $C(^3P)$ + C_2H_3 Reaction. The $C(^3P)$ + C_2H_3 reaction can produce C_3H_2 and C_3H products via C_3H_3 intermediate species by the mechanisms summarized at the following scheme:

Figure 5. CASSCF(11,11)/6-311+G(d,p) optimized geometry of the transition states of the $C(^3P)$ + C_2H_3 reaction on the first excited-state PES. Bond lengths are in Å and bond angles are in degrees. Symmetry of the species and their electronic states are also specified.
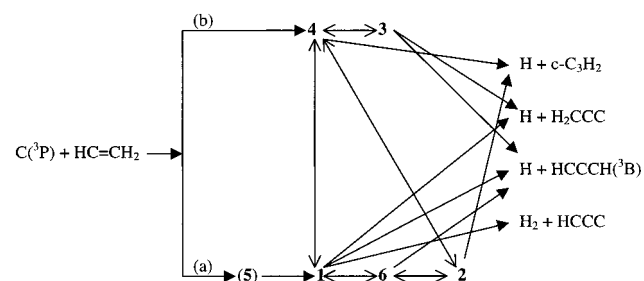
At the initial reaction step $C(^3P)$ + C_2H_3 can produce without entrance barrier isomers **4** and **5**, but the latter would immediately rearrange to **1**. Along channel a, there exist five pathways from **1** to the products. The barrier heights lie between 90.6 and 113.2 kcal/mol. The highest barrier relative to **1** is 113.2 kcal/mol for the **1** → **6** → H + HCCCH(^{3}B) path, and the lowest one is 90.6 kcal/mol for the **1** → **4** → **2** → H + c-C_3H_2 channel, 4−5 kcal/mol lower than the barriers for the other mechanisms such as **1** → H₂ + HCCC, **1** → H + HCCCH-(^{3}B), and **1** → H + H₂CCC. Among channel b, there are four feasible decay channels from **4** to the products. The **4** → **2** → H + c-C_3H_2 path is the most favorable and has a barrier of 50.5 kcal/mol with respect to **4**. The next favorable path is one-step **4** → H + c-C_3H_2 dissociation with a barrier of 53.0 kcal/
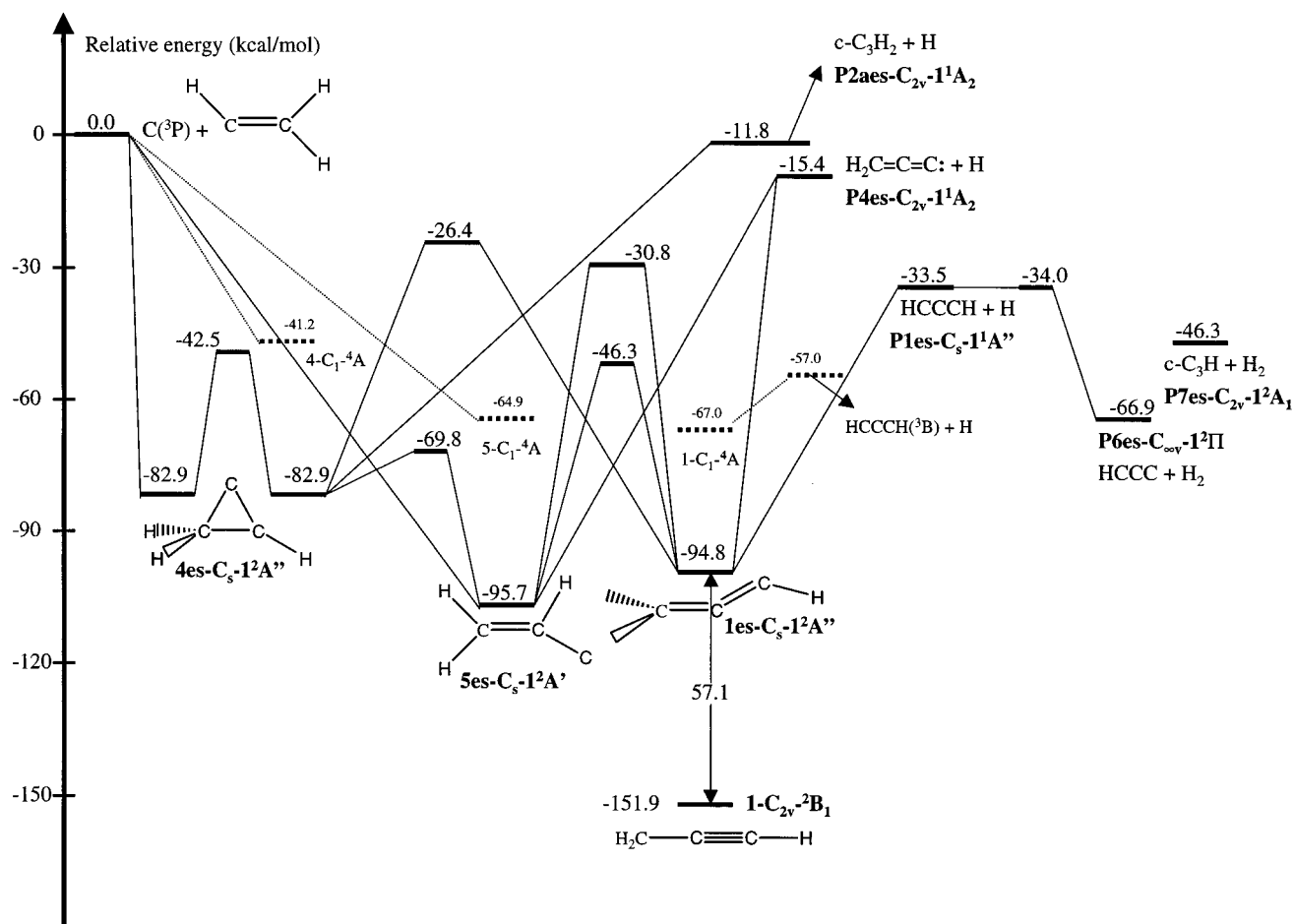
Figure 6. Potential energy diagram for the C(^{3}P) + C$_2$H$_3$ reaction on the first excited state PES. The relative energies are computed at the MRCI+D-(7,8)/ANO(2+)//CASSCF(11,11)/6-311+G(d,p) level of theory.

mol. The barrier heights for the other paths, **4** → **3** → H + H$_2$CCC and **4** → **1** → H$_2$ + HCCC, are only 2−5 kcal/mol higher.

Thus, the channels producing *c*-C$_3$H$_2$, such as **4** → **2** → H + *c*-C$_3$H$_2$, **4** → H + *c*-C$_3$H$_2$, and **1** → **4** → **2** → H + *c*-C$_3$H$_2$ have the most favorable energetics. Hence, *c*-C$_3$H$_2$ is expected to be the major dissociation product of C$_3$H$_3$. This conclusion agrees with the previous theoretical calculations by Vereecken et al.[5] and experimental results.[7,8] However, the energetics for other product pathways such as **4** → **3** → H + H$_2$CCC, **4** → **1** → H$_2$ + HCCC, **1** → H$_2$ + HCCC, **1** → H + HCCCH(^{3}B), and **1** → H + H$_2$CCC are 2−5 kcal/mol higher than those to yield H + *c*-C$_3$H$_2$. Therefore, detailed RRKM calculations will be needed to predict the product branching ratio.

4.2. First Excited-State PES. Besides channel 1, yielding C$_3$H$_3$ intermediate species on the ground electronic state PES, the C(^{3}P) + C$_2$H$_3$ reaction can also proceed following channel 2, producing C$_3$H$_3$(D$_1$) isomers on the first excited doublet state PES. The electronically excited C$_3$H$_3$ can undergo unimolecular rearrangements, dissociations to C$_3$H(D$_1$) and C$_3$H$_2$(S$_1$) by splitting H$_2$ and H, respectively, or internal conversion into the ground state.

4.2.1. Local Minima on First Excited-State PES. We have studied electronically excited C$_3$H$_2$ species earlier,[6] so we do not discuss them here. Geometry optimization for the C$_3$H$_3$ and *c*-C$_3$H isomers was carried out employing various levels of theory (see Figure 4). The first excited-state *c*-C$_3$H species has the same C$_{2v}$ symmetry as the ground state but has a 1^{2}A$_1$ electronic state instead of a 1^{2}B$_2$ state. Its geometry is in satisfactory agreement with that computed by Stanton[20] using

the EOMIP-CCSD/cc-pVTZ level of theory. While the C$_1$−C$_2$ bond distance does not change, the C$_2$−C$_3$ bond is about 0.17 Å longer in comparison with that in the ground state. This is a result of excitation of a π electron from the C$_2$=C$_3$ bond to the C$_1$ atom having an unpaired electron: the $n \leftarrow \pi$ transition. The vertical and adiabatic excitation energies for this transition are 26.85 (1.165 eV) and 23.18 (1.005 eV) kcal/mol, respectively, calculated utilizing the UCCSD(T)/6-311+G(3df,2p)//QCISD/6-311G(d,p) + ZPE[QCISD/6-311G(d,p)] level of theory. The latter is in good agreement with 0.949 eV determined by Stanton; the former is consistent with the experimental value of 1.240 eV reported by Yamamoto and Saito[21] and the theoretical results of 1.154 eV by Takahashi and Yamashita[22] and 1.18 eV by Ikuta.[46]

For excited-state C$_3$H$_3$ species, we only looked for isomers, from which low-lying excited-state C$_3$H and C$_3$H$_2$ species could be produced. We found three isomers: **1es**, **4es**, and **5es**. **1es**, the first excited state of **1**, has C$_s$ symmetry and 1^{2}A″ electronic state. Its structure resembles that of allenyl radical. The transfer of a π electron from the C$_1$≡C$_2$ triple bond of propargyl radical (H$_2$CCCH) to the C$_2$−C$_3$ bond elongates the C$_1$−C$_2$ bond distance but shortens the C$_2$−C$_3$ bond. This is also a $n \leftarrow \pi$ transition. Optimized geometry of **1es** is consistent with the previous result by Honjou et al.[13] The adiabatic excitation energy is 57.1 kcal/mol computed at the MRCI+D(7,8)/ANO(2+) level of theory, 21.5 kcal/mol lower than 78.6 kcal/mol derived using the MCSCF(5,5)/4-31G level in ref 13.

4es, the first excited state of **4**, has the same C$_s$ symmetry as the ground state but the 1^{2}A″ electronic state. Because of transfer of a π electron from C$_1$=C$_2$ to the C$_2$ atom with an unpaired

TABLE 4: Total Energy, $H_{298} - H_0$, Thermal Correction (TC) Calculated at G3, RCCSD(T)/6-311+G(3df,2p), and UCCSD(T)/6-311+G(3df,2p) Levels, and Heats of Formation of Different Reference Species

species	E_0(G3) (hartrees)	$H_{298} - H_0$(G3) (hartrees)	RCCSD(T) (hartrees)[b]	UCCSD(T) (hartrees)[b]	TC (kcal/mol)[b]	$\Delta H_f^o{}_{298}$ expt (kcal/mol)[c]
H$^+$	0	0	0	0	0	365.7
H•(^{2}S); <S^2> = 0.75[a]	−0.50100	0.00161	−0.49981	−0.49981	0	52.1
C(^{3}P)	−37.82772	0.00040			0	
:CH$_2$(C_{2v}-^{1}A$_1$)			−39.05892	−39.05892	12.12	102.7[d]
:CH$_2$(C_{2v}-^{3}B$_1$)				−39.07511	12.57	93.8[d]
CH$_3$•(D_{3h}-^{2}A″$_2$); <S^2> = 0.761[a]	−39.79329	0.00420	−39.75698	−39.75720	20.48	34.8
CH$_3^+$(D_{3h}-^{1}A′$_1$)	−39.43698	0.00379	−39.40044	−39.40044	21.35	261.7
CH$_3^-$(C_{3v}-^{1}A$_1$)			−39.75174	−39.75174	19.18	33.1 ± 0.9
CH$_4$(T_d-^{1}A$_1$)	−40.45761	0.00380	−40.43293	−40.43293	29.78	−17.9
CH$_4$•$^+$(C_{2v}-^{2}A$_1$)				−39.96098	24.81	
C$_2$H$_5$•(C_s-^{2}A′); <S^2> = 0.762[a]	−79.06397	0.00479	−78.99543	−78.99571	39.52	28.9
C$_2$H$_6$(D_{3d}-^{1}A$_{1g}$)	−79.72341	0.00434	−79.66603	−79.66603	48.86	−20.0
i-C$_3$H$_7$•(C_s-^{2}A′); <S^2> = 0.763[a]	−118.33814	0.00584	−118.23634	−118.23669	58.18	21.5
C$_3$H$_8$(C_{2v}-^{1}A$_1$)	−118.99390	0.00531	−118.90293	−118.90293	67.48	−25.0
HCCC•(C_s-^{2}A′)				−114.45636	13.17	
c-C$_3$H•(C_{2v}-^{2}B$_2$)				−114.46055	13.97	
H$_2$C=C=C:(C_{2v}-^{1}A$_1$)			−115.11133	−115.11133	21.80	
c-C$_3$H$_2$(C_{2v}-^{1}A$_1$)			−115.13405	−115.13405	22.09	
HCCCH(C_{2v}-^{1}A$_1$)				−115.09076	20.15	
HCCCH(C_2-^{3}B)				−115.10924	19.42	
H$_2$C•−C≡CH(C_{2v}-^{2}B$_1$); <S^2> = 0.973[a]	−115.91165	0.00500	−115.77402	−115.77519	28.24	
[H$_2$C−C≡CH]$^+$(C_{2v}-^{1}A$_1$)				−115.45997	−115.45997	29.25	
[H$_2$C−C≡CH]$^-$(C_s-^{1}A′)			−115.80539	−115.80539	27.63	
C$_3$H$_3$•(C_s-^{2}A′); <S^2> = 0.759[a] cyclopro-2-enyl radical	−115.85803	0.00424	−115.72546	−115.72585	28.64	
C$_3$H$_3^+$(D_{3h}-^{1}A′$_1$) cyclopro-2-enyl cation			−115.50609	−115.50609	30.24	
C$_3$H$_3^-$(C_s-^{1}A′) cyclopro-2-enyl anion			−115.70991	−115.70991	26.42	
C$_3$H$_3$•(C_s-^{2}A′); <S^2> = 0.940[a] cyclopro-1-enyl radical	−115.84316	0.00412	−115.71208	−115.71278	29.06	
C$_3$H$_3^-$(C_s-^{1}A′) cyclopro-1-enyl anion			−115.76692	−115.76692	28.01	
H$_3$C−C≡C•(C_{3v}-^{2}A$_1$); <S^2> = 1.129[a]	−115.84342	0.00469	−115.71178	−115.71247	28.60	
H$_3$C−C≡C$^+$(C_{3v}-^{1}A$_1$)	−115.35857	0.00435		−115.23092[e]	28.69[e]	
H$_3$C−C≡C$^-$(C_{3v}-^{1}A$_1$)	−115.94544	0.00460	−115.81037	−115.81037	29.13	
H$_3$C−C≡CH(C_{3v}-^{1}A$_1$)	−116.55536	0.00465	−116.43035	−116.43035	37.30	44.3
[H$_3$C−C≡CH]•$^+$(C_s-^{2}A′); <S^2> = 0.758[a]	−116.17380	0.00488		−116.05017	34.85	
H$_2$C=C=CH$_2$(D_{2d}-^{1}A$_1$)	−116.55426	0.00456	−116.42828	−116.42828	36.80	45.5
[H$_2$C=C=CH$_2$]•$^+$(D_2-^{2}B$_2$); <S^2> = 0.857[a]	−116.19785	0.00480		−116.07300	35.32	
c-C$_3$H$_4$(C_{2v}-^{1}A$_1$)	−116.51647	0.00411	−116.39324	−116.39324	37.09	66.2[d]
c-C$_3$H$_4$•$^+$(C_2-^{2}B); <S^2> = 0.759[a]	−116.15869	0.00440		−116.03662	33.98	

[a] Obtained at the UHF/6-31G(d) level. [b] Optimized geometry and TC were calculated at the B3LYP/6-311G(d,p) level. [c] From ref 30. [d] From ref 44. [e] Geometry optimized at the MP2/6-311G(d,p) and ZPE scaled by 0.95 (ref 63).

electron, the C$_1$−C$_2$ bond length increases. This is a $n \leftarrow \pi$ transition with the adiabatic excitation energy of 28.9 kcal/mol (1.253 eV) derived from the relative energies in Figures 3 and 6. **4es** lies 69.0 and 11.9 kcal/mol higher in energy than **1** and **1es**, respectively.

5es is the first excited state of **5**. It has a planar geometry, C_s symmetry and 1^{2}A′ electronic state. The $n \leftarrow \pi$ transition shortens the C$_2$−C$_3$ bond and elongates the C$_1$−C$_2$ bond. Consequently, the π bond moves along the molecule from the C$_1$=C$_2$ bond in the ground state to the C$_2$=C$_3$ bond in the excited state. The adiabatic excitation energy is only 9.3 kcal/mol (0.403 eV). Interestingly, this isomer is located 46.9 kcal/mol higher in energy than **1** on the ground-state PES but 0.9 kcal/mol lower than **1es** on the excited-state PES. Thus, **5es** is the most stable one of three isomers investigated here.

4.2.2. Transition States on the First Excited-State PES. Six transition states are found on the excited-state PES: **TS(1es/4es)**, **TS(1es/5es)a**, **TS(1es/5es)b**, **TS(4es/4es)**, **TS(4es/5es)**, and **TS(P1es/P6es)**. Except **TS(1es/4es)**, all of them have no symmetry. However, **TS(1es/5es)**, **TS(4es/5es)**, and **TS(P1es/P6es)** are nearly C_s symmetric. **TS(4es/4es)** is the transition state for degenerate isomerization of **4es** by 1,2-H migration. The

computed barrier height is 40.4 kcal/mol. The transformation of **4es** → **5es** occurs via **TS(4es/5es)** by a ring opening. **TS(4es/5es)** has similar geometry with that of **TS(4/5a)** in the ground state, but with longer bond distances in the C$_1$−C$_2$−C$_3$ cycle and larger C$_3$−C$_1$−C$_2$ angle. Among the transition states on the excited-state PES, **TS(4es/5es)** possesses the lowest energy (82.1 kcal/mol relative to **1**), 30.3 kcal/mol above **TS(4/5a)**. The barriers of 13.1 and 25.9 kcal/mol are calculated relative to the reactant and the product, respectively. **TS(1es/5es)a** is a transition state for the **5es** → **1es** channel, which occurs by a 1,2-H shift. Its structure is quite distinct from **TS(1/5)** on the ground-state PES. The C$_1$−C$_2$, C$_2$−C$_3$, and C$_2$−H$_1$ bonds are stretched, but the H$_1$−C$_2$−C$_1$ angle is reduced. The largest geometry change is a rotation of the CH$_2$ group (at C$_3$) by about 102° out the molecular plane. **TS(1es/5es)a** lies 74.5 kcal/mol above **TS(1/5)**. The barriers in the forward and reverse reactions are similar, 64−65 kcal/mol. We also found another transition state for the **1** → **5** channel, **TS(1es/5es)b**. Its structure is different from that of **TS(1es/5es)a**. The C$_1$−C$_2$ and C$_2$−H$_1$ bonds are longer, but the C$_2$−C$_3$ and C$_1$−H$_1$ bonds are shorter and the C$_1$−C$_2$−C$_3$ and H$_1$−C$_2$−C$_1$ angles are smaller. Consequently, **TS(1es/5es)b** is an earlier transition state

TABLE 5: Calculated Heats of Formation (at 298 K) for 2-Propynyl, Cycloprop-2-enyl, Cycloprop-1-enyl, and 1-Propynyl Radicals at the G3, RCCSD(T)/6-311+G(3df,2p), and UCCSD(T)/6-311+G(3df,2p) Levels of Theory

molecule	working reactions	G3 (kcal/mol)[a]	RCCSD(T) (kcal/mol)[a]	UCCSD(T) (kcal/mol)[a]	G3 (kcal/mol)[b] 0 K	G3 (kcal/mol)[b] 298 K	$\Delta H_f^o{}_{298}$(lit.) (kcal/mol)
H$_2$C•−C≡CH	(1) H$_2$C•−C≡CH + CH$_4$ → H$_3$C−C≡CH + CH$_3$•	84.0	84.9	84.3			85.2[c]
(C_{2v}-^{2}B$_1$)	(2) H$_2$C•−C≡CH + C$_2$H$_6$ → H$_3$C−C≡CH + C$_2$H$_5$•	83.3	84.5	84.0			81−86[e]
2-propynyl radical	(3) H$_2$C•−C≡CH + C$_3$H$_8$ → H$_3$C−C≡CH + i-C$_3$H$_7$•	83.1	84.6	84.1			81.5 ± 1[f]
	(4) H$_2$C•−C≡CH + CH$_4$ → H$_2$C=C=CH$_2$ + CH$_3$•	84.6	85.3	84.7	84.1	83.5	82.5 ± 3[g]
	(5) H$_2$C•−C≡CH + C$_2$H$_6$ → H$_2$C=C=CH$_2$ + C$_2$H$_5$•	83.8	84.9	84.4			83.6 ± 5.8[h]
	(6) H$_2$C•−C≡CH + C$_3$H$_8$ → H$_2$C=C=CH$_2$ + i-C$_3$H$_7$•	83.7	85.0	84.5			84.6[d]
	average: 1/N*Σ($\Delta H_f^o{}_{298}$)$_i$ with N = 6	83.8	84.9	84.3			
C$_3$H$_3$•	(7) C$_3$H$_3$•(cyc-2) + CH$_4$ → c-C$_3$H$_4$ + CH$_3$•	115.0	114.6	114.5			105.1 ± 4.1[i]
(C_s-2A′)	(8) C$_3$H$_3$•(cyc-2) + C$_2$H$_6$ → c-C$_3$H$_4$ + C$_2$H$_5$•	114.3	114.2	114.2	117.7	116.6	116.5[j]
cycloprop-2-enyl radical	(9) C$_3$H$_3$•(cyc-2) + C$_3$H$_8$ → c-C$_3$H$_4$ + i-C$_3$H$_7$•	114.1	114.4	114.3			
	average: 1/N*Σ($\Delta H_f^o{}_{298}$)$_i$ with N = 3	114.5	114.4	114.3			
C$_3$H$_3$•	(10) C$_3$H$_3$•(cyc-1) + CH$_4$ → c-C$_3$H$_4$ + CH$_3$•	124.3	123.5	123.2			
(C_s-^{2}A′)	(11) C$_3$H$_3$•(cyc-1) + C$_2$H$_6$ → c-C$_3$H$_4$ + C$_2$H$_5$•	123.5	123.1	122.8	127.1	125.9	
cycloprop-1-enyl radical	(12) C$_3$H$_3$•(cyc-1) + C$_3$H$_8$ → c-C$_3$H$_4$ + i-C$_3$H$_7$•	123.4	123.1	122.9			
	average: 1/N*Σ($\Delta H_f^o{}_{298}$)$_i$ with N = 3	123.7	123.2	123.0			
H$_3$C−C≡C•	(13) H$_3$C−C≡C• + CH$_4$ → H$_3$C−C≡CH + CH$_3$•	126.7	124.3	124.0			122.4 ± 3[g]
(C_{3v}-^{2}A$_1$)	(14) H$_3$C−C≡C• + C$_2$H$_6$ → H$_3$C−C≡CH + C$_2$H$_5$•	125.9	124.0	123.7	126.9	126.1	
1-propynyl radical	(15) H$_3$C−C≡C• + C$_3$H$_8$ → H$_3$C−C≡CH + i-C$_3$H$_7$•	125.8	124.0	123.8			
	average: 1/N*Σ($\Delta H_f^o{}_{298}$)$_i$ with N = 3	126.1	124.1	123.8			

[a] Calculated from the working reactions. [b] Computed from atomization energy. [c] $\Delta H_f^o{}_0$(H$_2$C•−C≡CH) from ref 25. [d] Derived from $\Delta H_f^o{}_0$(H$_2$C•−C≡CH) = 85.2 kcal/mol and the thermal correction of $\Delta H_f^o{}_{298}$(G3) − $\Delta H_f^o{}_0$(G3), 83.5−84.1, = −0.6 kcal/mol. [e] Theoretical values from ref 64. [f] From ref 37. [g] From ref 24. [h] From ref 23. [i] From ref 26. [j] From ref 29.

TABLE 6: Calculated IP, EA, PA, and C−H BDE for 2-Propynyl, Cycloprop-2-enyl, Cycloprop-1-enyl, and 1-Propynyl Radicals

molecule		reaction	method	ΔH(calcd)[a]	ΔH(lit.)
H$_2$C•−C≡CH	IP	(16) H$_2$C•−C≡CH → [H$_2$C−C≡CH]$^+$ + e$^-$	UCCSD(T)	198.8; 201.0[e]; 199.9[f]	199.5[g]; 199.9 ± 0.5[h]; 200.0[i]; 200.2
2-propynyl radical	EA	(17) [H$_2$C−C≡CH]$^-$ → H$_2$C•−C≡CH + e$^-$	UCCSD(T)	19.6; 23.2[b]; 22.9[c]; 23.5[d]	20.6 ± 0.6[k]; 21.2 ± 0.2[m]; 22.5[n]
(C_{2v}-^{2}B$_1$)	PA	(18a) [H$_3$C−C≡CH]•$^+$ → H$_2$C•−C≡CH + H$^+$	G3	164.6	
			UCCSD(T)	165.9; 167.6[p]; 166.8[f]	
		(18b) [H$_2$C=C=CH$_2$]•$^+$ → H$_2$C•−C≡CH + H$^+$	G3	179.7	177[l]
			UCCSD(T)	179.8; 181.4[p]; 180.6[f]	
	BDE	(19a) H$_2$C•−C≡CH → H$_2$C=C=C: + H•	UCCSD(T)	96.5; 96.6 (at 0 K); 100.2[o]	100 ± 5[m]
		(19b) H$_2$C•−C≡CH → HCCCH(^{1}A$_1$) + H•	UCCSD(T)	107.8; 111.5[o]	
		(19c) H$_2$C•−C≡CH → HCCCH(^{3}B) + H•	UCCSD(T)	95.4; 100.0[q]	
C$_3$H$_3$•	IP	(20) c-C$_3$H$_3$• → [c-C$_3$H$_3$]$^+$ + e$^-$	UCCSD(T)	139.5; 141.7[e]; 140.6[f]	152.2[l]
cycloprop-2-enyl radical	EA	(21) [c-C$_3$H$_3$]$^-$ → c-C$_3$H$_3$• + e$^-$	UCCSD(T)	−7.8; −4.2[b]; −4.5[c]; −3.9[d]	−4.1[t]
(C_s-^{2}A′)	PA	(22) [c-C$_3$H$_4$]•$^+$ → c-C$_3$H$_3$• + H$^+$	G3	188.6	175.5[l]
			UCCSD(T)	189.7; 191.3[p]; 190.5[f]	
	BDE	(23) c-C$_3$H$_3$• → c-C$_3$H$_2$ + H•	UCCSD(T)	51.2; 50.9 (at 0 K); 54.9[o]	53.7[r]
C$_3$H$_3$•	IP	none		none	
cycloprop-1-enyl radical	EA	(24) [c-C$_3$H$_3$]$^-$ → c-C$_3$H$_3$• + e$^-$	UCCSD(T)	35.0; 38.6[b]; 38.3[c]; 38.9[d]	
(C_s-^{2}A′)	PA	(25) [c-C$_3$H$_4$]•$^+$ → c-C$_3$H$_3$• + H$^+$	G3	197.8	
			UCCSD(T)	198.3; 199.9[p]; 199.1[f]	
	BDE	(26) c-C$_3$H$_3$• → c-C$_3$H$_2$ + H•	UCCSD(T)	42.6; 42.5 (at 0 K); 46.3[o]	
H$_3$C−C≡C•	IP	(27) H$_3$C−C≡C• → [H$_3$C−C≡C]$^+$ + e$^-$	G3	304.0	
1-propynyl radical			UCCSD(T)	302.3	
(C_{3v}-^{2}A$_1$)	EA	(28) [H$_3$C−C≡C]$^-$ → H$_3$C−C≡C• + e$^-$	G3	64.1	(>60.0)[k]; 62.7 ± 0.2[m]; 64.6 ± 5.5[s]
			UCCSD(T)	60.9; 64.5[b]; 64.2[c]; 64.8[d]	
	PA	(29) [H$_3$C−C≡CH]•$^+$ → H$_3$C−C≡C• + H$^+$	G3	207.2	
			UCCSD(T)	205.7; 207.3[p]; 206.5[f]	
	BDE	(30) H$_3$C−C≡C• → H$_2$C=C=C: + H•	UCCSD(T)	56.8; 56.3 (at 0 K); 60.5[o]	

[a] From the working reaction (all in kcal/mol, at 298 K unless noted otherwise). [b] Evaluated from $\Delta H_f^o{}_{298}$(C$_3$H$_3$•) in Table 5 and $\Delta H_f^o{}_{298}$(C$_3$H$_3^-$) in Table 7. [c] Derived from the working reaction including "higher level correction"[54a]: HLC = −5.25n$_\beta$ − 0.19n$_\alpha$. [d] Computed from ΔH_r of C$_3$H$_3^-$ + CH$_3$• → C$_3$H$_3$• + CH$_3^-$ and the experimental EA(CH$_3$•) value of 1.8 ± 0.7 kcal/mol; ref 30. [e] Calculated from ΔH_r of C$_3$H$_3$• + CH$_3^+$ → C$_3$H$_3^+$ + CH$_3$• and the experimental IP(CH$_3$•) value of 226.9 ± 0.2 kcal/mol; ref 30. [f] Average value. [g] From ref 11. [h] From ref 12a. [i] From ref 15. [j] From ref 12b. [k] From ref 32. [l] From ref 31. [m] From ref 24. [n] From ref 33. [o] Derived from ΔH_r of C$_3$H$_3$• + :CH$_2$(^{1}A$_1$) → C$_3$H$_2$ + CH$_3$• and the experimental ΔH_r of CH$_3$• → :CH$_2$(^{1}A$_1$) + H•, 119.9 kcal/mol. [p] Calculated from ΔH_r of C$_3$H$_4$•$^+$ + :CH$_2$(^{1}A$_1$) → C$_3$H$_3$• + CH$_3^+$ and the experimental ΔH_r of CH$_3^+$ → :CH$_2$(^{1}A$_1$) + H$^+$, 206.7 kcal/mol. [q] Derived from ΔH_r of H$_2$C•−C≡CH + :CH$_2$(^{3}B$_1$) → HCCCH(^{3}B) + CH$_3$• and the experimental ΔH_r of CH$_3$• → :CH$_2$(^{3}B$_1$) + H•, 111.0 kcal/mol. [r] From ref 16. [s] From ref 34. [t] From ref 29.

than **TS(1es/5es)a** and corresponds to a barrier 15.5 kcal/mol lower than that at **TS(1es/5es)a**. Isomerization of **4es** → **1es** takes place by a ring opening. The corresponding transition state

TS(1es/4es) has the same C_s symmetry as **TS(1/4)** in the ground state but a 1^{2}A″ electronic state. Its geometry changes significantly. The $n ← \pi$ transition elongates the C$_2$−C$_3$ bond from

TABLE 7: Calculated $\Delta H_f^o{}_{298}$ for 2-Propynyl Cation, 2-Propynyl Anion, Cycloprop-2-enyl Cation, Cycloprop-2-enyl Anion, Cycloprop-1-enyl Anion, 1-Propynyl Cation, and 1-Propynyl Anion from $\Delta H_{r,298}$

species	working reaction	$\Delta H_{r,298}$ (kcal/mol)	$\Delta H_f^o{}_{298}$(calcd) (kcal/mol)	method	$\Delta H_f^o{}_{298}$(lit.) (kcal/mol)
$[H_2C-C\equiv CH]^+$	(31) $[H_2C-C\equiv CH]^+ + CH_4 \rightarrow H_3C-C\equiv CH + CH_3^+$	38.6	285.3	UCCSD(T)	281.8[a]; 282.0[b]; 284.6[f]
	(32) $[H_2C-C\equiv CH]^+ + CH_4 \rightarrow H_2C=C=CH_2 + CH_3^+$	39.4	285.7	UCCSD(T)	
	average: $1/N^*\Sigma(\Delta H_f^o{}_{298})_i$ with $N = 2$		285.5		
$[H_2C-C\equiv CH]^-$	(33) $[H_2C-C\equiv CH]^- + CH_4 \rightarrow H_3C-C\equiv CH + CH_3^-$	34.4	60.9	UCCSD(T)	61.3 ± 3.2[e]; 60.5 ± 2.2[h]
	(34) $[H_2C-C\equiv CH]^- + CH_4 \rightarrow H_2C=C=CH_2 + CH_3^-$	35.2	61.3	UCCSD(T)	
	average: $1/N^*\Sigma(\Delta H_f^o{}_{298})_i$ with $N = 2$		61.1		
$[c\text{-}C_3H_3]^+$ cycloprop-2-enyl cation	(35) $[c\text{-}C_3H_3]^+ + CH_4 \rightarrow c\text{-}C_3H_4 + CH_3^+$	89.6	256.2	UCCSD(T)	254[b]; 256 ± 2[c]; 256.7[d]; 257.3 ± 0.8[a]
$[c\text{-}C_3H_3]^-$ cycloprop-2-enyl anion	(36) $[c\text{-}C_3H_3]^- + CH_4 \rightarrow c\text{-}C_3H_4 + CH_3^-$	−1.3	118.5	UCCSD(T)	110−122.3[d]
$[c\text{-}C_3H_3]^-$ cycloprop-1-enyl anion	(37) $[c\text{-}C_3H_3]^- + CH_4 \rightarrow c\text{-}C_3H_4 + CH_3^-$	32.9	84.3	UCCSD(T)	
$[H_3C-C\equiv C]^+$	(38) $[H_3C-C\equiv C]^+ + CH_4 \rightarrow H_3C-C\equiv CH + CH_3^+$	−106.4	430.3	G3	
		−104.6	428.5	UCCSD(T)	
$[H_3C-C\equiv C]^-$	(39) $[H_3C-C\equiv C]^- + CH_4 \rightarrow H_3C-C\equiv CH + CH_3^-$	36.0	59.3	UCCSD(T)	59.9 ± 2.2[g]; 59.7 ± 3[e]

[a] From ref 31. [b] From ref 35. [c] From ref 12b. [d] From ref 29. [e] From ref 24. [f] From IP($H_2C^\bullet\text{-}C\equiv CH$) = 200 kcal/mol and $\Delta H_f^o{}_{298}(H_2C^\bullet\text{-}C\equiv CH)$ = 84.6 kcal/mol. [g] From ref 34. [h] From ref 32.

TABLE 8: Calculated IP, C−H BDE, and GPA for Propyne ($H_3C-C\equiv CH$), Allene ($H_2C=C=CH_2$), and Cyclopropene ($c\text{-}C_3H_4$)

molecule		reaction	method			
			G3[a]	UCCSD(T)[a]	UCCSD(T)	lit.
$H_3C-C\equiv CH$	IP	(40) $H_3C-C\equiv CH \rightarrow [H_3C-C\equiv CH]^{\bullet+} + e^-$	239.4 (0 K); 239.5	236.1	235.7[e]; 239.4[d]	238.9[g]
propyne	BDE	(41) $H_3C-C\equiv CH \rightarrow H_3C-C\equiv C^\bullet + H^\bullet$	132.4 (0 K); 133.4	128.1	131.8[b]; 131.4[d]; 131.6[f]	130.2 ± 3[h]; 135.9 ± 2[k]
(C_{3v}-$^1A_1$)		(42) $H_3C-C\equiv CH \rightarrow H_2C^\bullet\text{-}C\equiv CH + H^\bullet$	89.6 (0 K); 90.8	88.4	92.0[b]; 91.6[d]; 92.1[f]	89.3[m]; 90.6[n]; 90.3 ± 3[h]
	GPA	(43) $H_3C-C\equiv CH \rightarrow [H_2C-C\equiv CH]^- + H^+$		382.5	382.3[c]	382.3 ± 1.2[i]; 382.7 ± 3[h]; 383.2[l]
		(44) $H_3C-C\equiv CH \rightarrow [H_3C-C\equiv C]^- + H^+$		380.9	380.7[c]	381.0 ± 2.1[j]; 381.1 ± 3[h]; 382.1[l]
$H_2C=C=CH_2$	IP	(45) $H_2C=C=CH_2 \rightarrow [H_2C=C=CH_2]^{\bullet+} + e^-$	223.7 (0 K); 223.8	221.5	221.1[e]; 224.8[d]	223.4[o]; 223.5[g]
allene	BDE	(46) $H_2C=C=CH_2 \rightarrow H_2C^\bullet\text{-}C\equiv CH + H^\bullet$	88.9 (0 K); 90.2	87.6	91.2[b]; 90.8[d]; 90.9[f]	88.7 ± 3[h]
(D_{2d}-$^1A_1$)	GPA	(47) $H_2C=C=CH_2 \rightarrow [H_2C-C\equiv CH]^- + H^+$		381.7	381.5[c]	381.1 ± 3[h]; 380.6 ± 2.1[i]
$c\text{-}C_3H_4$	IP	(48) $c\text{-}C_3H_4 \rightarrow [c\text{-}C_3H_4]^{\bullet+} + e^-$	224.5 (0 K); 224.7	220.7	220.3[e]; 224.0[d]	223[g]
cyclopropene	BDE	(49) $c\text{-}C_3H_4 \rightarrow c\text{-}C_3H_3^\bullet(\text{cyc-2}) + H^\bullet$	98.8 (0 K); 99.9	96.7	100.3[b]; 99.9[d]; 100.2[f]	99[p]
(C_{2v}-$^1A_1$)		(50) $c\text{-}C_3H_4 \rightarrow c\text{-}C_3H_3^\bullet(\text{cyc-1}) + H^\bullet$	108.1 (0 K); 109.1	105.2	109.0[b]; 108.4[d]; 108.9[f]	
	GPA	(51) $c\text{-}C_3H_4 \rightarrow c\text{-}C_3H_3\text{-}(\text{cyc-2}) + H^+$		418.2	418.0[c]	
		(52) $c\text{-}C_3H_4 \rightarrow c\text{-}C_3H_3\text{-}(\text{cyc-1}) + H^+$		384.0	383.8[c]	

[a] Derived from the working reaction (all in kcal/mol, at 298 K unless indicated otherwise). [b] Calculated from ΔH_r of $C_3H_4 + H_3C^\bullet \rightarrow C_3H_3^\bullet + CH_4$ and the experimental BDE(H_3C-H) value of 104.7 ± 0.1 kcal/mol; ref 30. [c] Evaluated from ΔH_r of $C_3H_4 + H_3C^- \rightarrow C_3H_3^- + CH_4$ and the experimental GPA(H_3C-H) value of 416.7 ± 0.8 kcal/mol; ref 30. [d] Computed from ΔH_r of the working reaction including "higher level correction"[54a]: HLC = $-5.25n_\beta - 0.19n_\alpha$. [e] Derived from ΔH_r of $C_3H_4 + CH_4^{\bullet+} \rightarrow C_3H_4^{\bullet+} + CH_4$ and the experimental IP(CH_4) value of 290.8 ± 0.2 kcal/mol. [f] Calculated from $\Delta H_f^o{}_{298}(C_3H_4)$, $\Delta H_f^o{}_{298}(H^\bullet)$ and $\Delta H_f^o{}_{298}(C_3H_3^\bullet)$, computed at the UCCSD(T)/6-311+G(3df,2p) level. [g] From ref 31. [h] From ref 24. [i] From ref 32. [j] From ref 34. [k] From ref 65. [l] From ref 59. [m] From ref 36. [n] From ref 37. [o] From ref 38. [p] From ref 16.

TABLE 9: Calculated $\Delta H_f^o{}_{298}$ for $c\text{-}C_3H_2$, $H_2C=C=C$, HCCCH(^3B), HCCCH($^1A_1$), HCCC$^\bullet$, and $c\text{-}C_3H^\bullet$ from $\Delta H_{r,298}$

species	working reaction	$\Delta H_{r,298}$ (kcal/mol)	$\Delta H_f^o{}_{298}$(calcd) (kcal/mol)	$\Delta H_f^o{}_{298}$(lit.) (kcal/mol)
$c\text{-}C_3H_2$	(53) $c\text{-}C_3H_2 + CH_4 \rightarrow c\text{-}C_3H_4 + :CH_2(^1A_1)$	69.4	117.4	114 ± 4[b] 119.5 ± 2.2[c]
$H_2C=C=C:$	(54) $H_2C=C=C: + CH_4 \rightarrow H_2C=C=CH_2 + :CH_2(^1A_1)$	33.1	132.9	129 ± 4[b]
HCCCH(^3B)	(55) HCCCH(^3B) + $CH_4 \rightarrow H_2C=C=CH_2 + :CH_2(^3B_1)$	24.5	132.7	132.2[d]
HCCCH($^1A_1$)	(56) HCCCH($^1A_1$) + $CH_4 \rightarrow H_2C=C=CH_2 + :CH_2(^1A_1)$	21.9	144.2	140[b]
HCCC$^\bullet$	(57) HCCC$^\bullet$ + $CH_4 \rightarrow H_2C^\bullet\text{-}C\equiv CH^a + :CH_2(^1A_1)$	32.1	172.8	
	(58) HCCC$^\bullet$ + $CH_4 \rightarrow H_3C-C\equiv C^\bullet a + :CH_2(^1A_1)$	71.8	172.6	
	average: $1/N^*\Sigma(\Delta H_f^o{}_{298})_i$ with $N = 2$		172.7	
$c\text{-}C_3H^\bullet$	(59) $c\text{-}C_3H^\bullet$ + $CH_4 \rightarrow c\text{-}C_3H_3^\bullet(\text{cyc-2})^a + :CH_2(^1A_1)$	65.2	169.7	
	(60) $c\text{-}C_3H^\bullet$ + $CH_4 \rightarrow c\text{-}C_3H_3^\bullet(\text{cyc-1})^a + :CH_2(^1A_1)$	73.8	169.8	
	average: $1/N^*\Sigma(\Delta H_f^o{}_{298})_i$ with $N = 2$		169.8	

[a] Taken from the previous calculations in Table 5. $\Delta H_f^o{}_{298}$ for $H_2C^\bullet-C\equiv CH$, $c\text{-}C_3H_3^\bullet$ (cyclopro-2-enyl radical), $c\text{-}C_3H_3^\bullet$ (cyclopro-1-enyl radical) and $H_3C-C\equiv C^\bullet$ are 84.3, 114.3, 123.0, and 123.8 kcal/mol, respectively. [b] From ref 28. [c] From ref 39. [d] From ref 45.

1.245 to 1.553 Å but shortens the C_1-C_2 bond from 1.489 to 1.418 Å. The C_3-C_1 breaking bond distance also increases by about 0.1 Å. The relative energy of **TS(1es/4es)** is 125.5 kcal/mol with respect to **1**, 43.4 kcal/mol higher than that of **TS-(4es/5es)**. Hence, opening the cycle at the C_2-C_3 bond is more

favorable in energy than at the C_1-C_3 bond, although the C_1-C_3 bond is about 0.13 Å longer. This contrasts with the ground-state PES where **TS(4/1)** is much lower than **TS(4/5)**.

When we tried to look for the transition state of H_2 elimination from **1es**, we found **TS(P1es/P6es)**, a transition state for the

P1es(HCCCH) + H → **P6es**(HCCC) + H$_2$ abstraction channel. **TS(P1es/P6es)** lies 0.5 kcal/mol lower in energy than the reactant, **P1es** + H at the MRCI+D(7,8)/ANO(2+) level, but 1.2 kcal/mol higher at the MRCI(7,8)/ANO level of theory. So, the **P1es** + H → **P6es** + H$_2$ reaction might not have a barrier.

We could not find transition states for H elimination from **1es**, **4es**, and **5es**. The search of transition states for H loss leads to dissociation of H. H$_2$ elimination pathways were not detected on the excited-state PES.

4.2.3. Mechanisms of the C(^{3}P) + C$_2$H$_3$ Reaction Involving Excited C$_3$H$_3$. Isomers **4es** and **5es**, formed in the C(^{3}P) + C$_2$H$_3$ reaction, are vibrationally excited. They can dissociate directly or isomerize to **1es**. Starting from **4es**, the reaction can follow the **4es** → **TS(4es/5es)** → **5es** → **TS(1es/5es)b** → **1es** path to reach **1es**. **4es** can directly lose a H atom producing excited c-C$_3$H$_2$(1^{1}A$_2$) **P2aes**, but this path is energetically unfavorable, since the latter lies 140.1 kcal/mol above **1** and only 11.8 kcal/mol below the reactants. **5es** directly dissociates by H elimination to **P4es**. **1es** can yield **P4es** and **P1es** by H splitting as well. The pathway producing **P1es** is more favorable energetically. The energy required is 61.3 kcal/mol, 18.1 kcal/mol lower than that of the **1es** → **P4es** + H route.

Formation of C$_3$H from electronically excited C$_3$H$_3$ must occur by a two-step process. A C−H bond in **1es** can be broken to give **P1es**, which then produces C$_3$H (**P6es**) by H abstraction. This however cannot occur under single collision conditions.

In summary, the C(^{3}P) + C$_2$H$_3$ reaction can yield electronically excited C$_3$H$_3$ isomers **4es** and **5es**, which then interconvert to **1es**. The C−H bond cleavage in **1es** leads to **P1es** (HCCCH, 1^{1}A$''$). This is the most energetically favorable channel.

4.3. Calculations of Thermochemical Parameters. Since C$_3$H$_3$ radicals are highly reactive intermediates, thermochemical data for them are not easily characterized by experimental measurements. The use of ab initio calculations, performed at high levels of theory, becomes suitable in this case. Previous investigations by Radom and co-workers[60] indicated that if the spin-contamination for radicals is moderate (<S^2> less than 1.0), B3LYP/6-31G(d) geometry optimization and vibrational frequencies can be utilized to compute thermochemical properties. As seen Table 4, C$_3$H$_3$ radicals in most cases satisfy this condition. The CCSD(T)/6-311+G(3df,2p)//B3LYP calculational scheme has been shown[53,54] to give accuracies of 1−2 kcal/mol for the atomization energies of the G2 test of molecules. Thus, the use of the CCSD(T)/6-311+G(3df,2p)//B3LYP/6-311G(d,p) + TC[B3LYP/6-311G(d,p)] level of theory in combination with the isodesmic approach allows us to reliably predict thermochemical data for the C$_3$H$_3$ radicals. For comparison, the G3 theory by Pople and co-workers[49] is also used. Where possible, computed values are compared to available experimental data as well.

4.3.1. Thermochemistry of C$_3$H$_3$ Radicals. 4.3.1.1. Heats of Formation. Calculated heats of formation ($\Delta H_f^o{}_{298}$) for C$_3$H$_3$ radicals are presented in Table 5. $\Delta H_f^o{}_{298}$(**1**) for 2-propynyl (propargyl) radical (isomer **1**) are derived either from six different working reactions using the G3, RCCSD(T), and UCCSD(T) levels or from atomization energies utilizing the G3 theory. The $\Delta H_f^o{}_{298}$ values obtained from different working reactions all lie within a range of 0.7 kcal/mol. Taking the average of the computed $\Delta H_f^o{}_{298}$ as our best estimate, the $\Delta H_f^o{}_{298}$ values of 83.8, 84.9, and 84.3 kcal/mol can be proposed using the G3, RCCSD(T), and UCCSD(T) methods, respectively. Those agree well with the $\Delta H_f^o{}_{298}$ value of 83.5 kcal/mol derived based on the G3 theory from atomization energies. Our results agree well with the previous theoretical value of

$\Delta H_f^o{}_{298}$ = 83.6 ± 5.8 kcal/mol at the BAC-MP4 level[23] and the experimental $\Delta H_f^o{}_{298}$ values of 82.5 ± 3 kcal/mol[24] and 85.2 kcal/mol (at 0 K).[25] If we take a thermal correction of −0.6 kcal/mol at the G3 level (Table 5) for the $\Delta H_f^o{}_0$(**1**) = 85.2 kcal/mol, we match the value of 84.6 kcal/mol for the experimental heat of formation of propargyl radical at 298 K. From the theoretical calculations and experimental data, we recommend $\Delta H_f^o{}_{298}$(propargyl radical) = 84.5 ± 1 kcal/mol.

Experimental $\Delta H_f^o{}_{298}$ for cycloprop-2-enyl radical (isomer **2**) reported earlier[26] based on ICR proton-transfer measurements is 105.1 ± 4.1 kcal/mol. However, the structure characterized by ICR proton transfer is inconsistent with that determined by ESR and ab initio calculations.[27,28] Hence, the value of 105.1 ± 4.1 kcal/mol was thought to be not accurate.[28] Recent G2 calculations[29] gave the value of 116.5 kcal/mol, which was derived by taking the average of the values from atomization energy and isodesmic reaction. Considering the large discrepancy (11.4 kcal/mol) and importance of accurate $\Delta H_f^o{}_{298}$(**2**) data for **2**, we proceed to recalculate the heat of formation for cycloprop-2-enyl radical. After taking the average from three isodesmic reactions, we obtain 114.5, 114.4, and 114.3 kcal/mol at the G3, RCCSD(T), and UCCSD(T) levels, respectively. From atomization energy using the G3 theory, $\Delta H_f^o{}_{298}$(**2**) is calculated as 117.7 and 116.6 kcal/mol at 0 and 298 K, respectively. The latter is in good agreement with 116.5 kcal/mol deduced by Glukhovtsev[29] but about 2.2 kcal/mol above the $\Delta H_f^o{}_{298}$(**2**) values evaluated from the isodesmic reactions. In general, the results derived from the isodesmic reactions are more reliable, so we recommend the value of 114.3 kcal/mol for the heat of formation of cycloprop-2-enyl radical.

Enthalpies of formation for cycloprop-1-enyl and 1-propynyl radicals are also calculated from either three different working reactions or atomization energies. Our best estimated values, taken as the average of those, are 123.7, 123.2, and 123.0 kcal/mol for the $\Delta H_f^o{}_{298}$ of cycloprop-1-enyl radical (isomer **4**) and 126.1, 124.1, and 123.8 kcal/mol for the $\Delta H_f^o{}_{298}$ of 1-propynyl radical (isomer **3**) at the G3, RCCSD(T), and UCCSD(T) methods, respectively. $\Delta H_f^o{}_{298}$ values for isomer **4** are in good agreement with each other, but the $\Delta H_f^o{}_{298}$ values for isomer **3** are not consistent. C$_{3v}$ structure of **3** has high spin-contamination (<S^2> is 1.13 at UHF/6-31G(d)); therefore, G3 involving MP2 calculations for basis set corrections may not be as accurate. The $\Delta H_f^o{}_{298}$(**3**) = 123.8 kcal/mol obtained at the UCCSD(T) level agrees well with the experimental value of 122.4 ± 3 kcal/mol reported by Robinson et al.[24]

Although the $\Delta H_f^o{}_{298}$(**1**) calculated from the atomization energy is consistent with that estimated from various isodesmic reactions, $\Delta H_f^o{}_{298}$(**2**), $\Delta H_f^o{}_{298}$(**3**), and $\Delta H_f{}_{298}$(**4**) derived from atomization energy deviate from those derived from different reactions overestimating them by about 2 kcal/mol. $\Delta H_f^o{}_{298}$ values based on the isodesmic approach are in closer agreement with experiment.

4.3.1.2. IP, EA, PA, and BDE for C$_3$H$_3$ Radicals. Ionization potential (IP): IP of C$_3$H$_3$ radicals is calculated using either the enthalpy of the unmediated C$_3$H$_3$ → C$_3$H$_3{}^+$ + e$^-$ reaction or the enthalpy of the isodesmic C$_3$H$_3$ + CH$_3{}^+$ → C$_3$H$_3{}^+$ + CH$_3$ reaction and the experimental IP(CH$_3$·) value of 226.9 ± 0.2 kcal/mol[30] (Table 6). The computed IP(**1**) values are 198.8 and 201.0 kcal/mol, based on the unmediated and isodesmic reactions, respectively. Taking the average of two values, we obtain the value of 199.9 kcal/mol (8.67 eV). This excellently agrees with the previous theoretical calculated IP(**1**) = 199.5 kcal/mol (8.65 eV) by Botschwina et al.[11] and the experimental IP(**1**) values of 200.2 kcal/mol (8.68 eV) by Lossing,[12b] 199.9

kcal/mol (8.67 eV) by Minsek,[12a] and 200.0 kcal/mol (8.673 eV) by Gillbert et al.[15]

Similarly, on the basis of the unmediated and isodesmic reactions mentioned above, the values of 139.5 and 141.7 kcal/mol are derived for the IP of cycloprop-2-enyl radical (isomer **2**). Our recommended IP(**2**), taken as the average, is 140.6 kcal/mol. It deviates by 11.6 kcal/mol from the experimental IP(**2**) = 152.2 kcal/mol.[31] This indicates that the experimental result may not be accurate.

The cycloprop-1-enyl cation was not located at the MP2/6-31G(d) and B3LYP/6-311G(d,p) levels of theory; hence, we did not compute IP for the cycloprop-1-enyl radical. Finally, the IP value for the propynyl radical is calculated as 304.0 and 302.3 kcal/mol at the G3 and UCCSD(T) levels of theory, respectively.

Electron affinity (EA): EA for C_3H_3 radicals can be calculated by four different ways: from the heat of unmediated $C_3H_3^- \rightarrow C_3H_3 + e^-$ reaction, from $\Delta H_f^o{}_{298}(C_3H_3)$ in Table 5 and $\Delta H_f^o{}_{298}(C_3H_3^-)$ in Table 7, from the heat of the same reaction including "higher level correction"[54a] (HLC = $-5.25n_\beta - 0.19n_\alpha$), and from the enthalpy of the $C_3H_3^- + CH_3 \rightarrow C_3H_3 + CH_3^-$ reaction and the experimental EA(CH$_3$•) = 1.8 ± 0.7 kcal/mol.[30] The computed EA values are 19.6, 23.2, 22.9, and 23.5 kcal/mol for isomer **1**; -7.8, -4.2, -4.5, and -3.9 kcal/mol for isomer **2**; 35.0, 38.6, 38.3 and 38.9 kcal/mol for isomer **4**; and 60.9, 64.5, 64.2 and 64.8 kcal/mol for isomer **3**. The computed EA(**1**) values are in close agreement with the experimental EA values of 20.6 kcal/mol by Oakes et al.,[32] 21.2 kcal/mol by Robinson et al.,[24] and the theoretical value of EA(**1**) = 22.5 kcal/mol by Ikuta.[33] EA(**3**) agrees well with the experimental values of 62.7 kcal/mol by Robinson and 64.6 kcal/mol by Bartmess et al.[34]

As seen in the Table 6, the EA values calculated from the enthalpies of unmediated reactions are about 3 kcal/mol lower than the remaining EA, which agree well experiment. Therefore, the EA values derived from isodesmic reactions are more reliable, mainly due to the fact that the number of electron pairs is not conserved when an electron is added.

It is worth mentioning that the calculated EA(**2**) values are negative. This agrees with previous result by Glukhovtsev et al.[29] and implies that the cyclopropenyl anion is not bound in the gas phase.[29]

Proton affinity (PA): PA for C_3H_3 radicals is computed either directly from the enthalpy of the $C_3H_4^{•+} \rightarrow C_3H_3 + H^+$ reaction or indirectly from the heat (ΔH_r) of the $C_3H_4^{•+} + :CH_2(^1A_1) \rightarrow C_3H_3 + CH_3^+$ reaction and the experimental ΔH_r = 206.7 kcal/mol[30] for the $CH_3^+ \rightarrow :CH_2(^1A_1) + H^+$ reaction. After taking the average of two computed values, we suggest the PA values of 166.8 kcal/mol for isomer **1** (to propynyl radical cation), 180.6 kcal/mol for **1** (to allenyl radical cation), 199.1 kcal/mol for **4**, and 206.5 kcal/mol for **3**. To collate with available experimental data, we choose the estimated PA from UCCSD(T)/6-311+G(3df,2p) calculations. While the computed PA(**1**) is in close agreement with that of 177 kcal/mol from the experiment,[31] the calculated PA(**2**) lies about 15 kcal/mol higher in energy. As for the case of IP(**2**), PA(**2**) depends on the heat of formation of the cycloprop-2-enyl radical, for which the experimental value is most likely erroneous.

C−H bond dissociation energy (BDE): BDEs can be also derived either directly from the $C_3H_3 \rightarrow C_3H_2 + H$ reaction or indirectly (Table 6). The indirectly obtained BDEs are about 3.7 kcal/mol higher than those derived from unmediated H additions although the number of electron pairs does not change. For comparison with experimental data, we choose the indirectly

computed BDEs since they usually provide a better agreement. The calculated BDE(H$_2$CC≡C−H) = 100.2 kcal/mol excellently agrees with the experimental BDE = 100 ± 5 kcal/mol by Robinson et al.,[24] and the computed BDE(*c*-C$_3$H$_2$−H) = 54.9 kcal/mol is close to the reliable CBS-QCI/APNO result (53.7 kcal/mol) of Montgomery et al.[16] The other proposed BDE values are the following: 111.5 [to HCCCH($^1A_1$)] and 100.0 kcal/mol [to HCCCH(^3B)] for H−CHC≡CH isomer, 46.3 kcal/mol for isomer **4**, and 60.5 kcal/mol for H−H$_2$CCC. The results indicate that the highest BDE is 111.5 kcal/mol for the fission of the CH bond (from CH$_2$ group) in isomer **1** to HCCCH($^1A_1$) and the lowest BDE is 46.3 kcal/mol for H splitting from **4**. In propargyl radical, the energy needed for breaking the CH bond of the CCH group is similar to that of splitting the CH bond of the H$_2$CC group [to HCCCH(^3B)], about 100 kcal/mol. This is 40−45 kcal/mol higher than the BDE for cycloprop-2-enyl and 1-propynyl radicals.

4.3.1.3. Enthalpies of Formation for Charged C$_3$H$_3$ Species. After adding or losing an electron, C_3H_3 radicals become anions or cations with even number of electrons. Therefore, the charged C_3H_3 species are more stable and easily characterized by the experimental measurements. Consequently, a lot of experimental data are available for the heats of formation of charged C_3H_3 (Table 7). These experimental results give us a good chance to further test the methods used in this paper. The heats of formation recommended by us are 285.5, 61.1, 256.2, 118.5, 84.3, and 59.3 kcal/mol for propargyl cation, propargyl anion, cyloprop-2-enyl cation, cyloprop-2-enyl anion, cyloprop-1-enyl anion, and 1-propynyl anion, respectively. While $\Delta H_f^o{}_{298}$ values for propargyl anion, cyloprop-2-enyl cation, and 1-propynyl anion are well consistent with experiment,[12b,24,31,32,34] $\Delta H_f^o{}_{298}$ for propargyl cation is about 3.5 kcal/mol higher than the experimental result recommended by Lias et al.[31] and the previous theoretical value by Li et al.[35] However, these experimental and theoretical values were derived from the experimental $\Delta H_f^o{}_{298}$(propargyl radical) = 81.5 ± 1 kcal/mol,[36,37] which lies 3 kcal/mol below our new value of 84.5 ± 1 kcal/mol and the experimental $\Delta H_f^o{}_{298}$(propargyl radical) = 84.6 kcal/mol by Roth et al.[25] (Table 5). If we take IP(propargyl radical) = 200.0 kcal/mol[15] and $\Delta H_f^o{}_{298}$(propargyl radical) = 84.5 kcal/mol, $\Delta H_f^o{}_{298}$(propargyl cation) is 284.5 kcal/mol. This value of 284.5 kcal/mol, proposed as the new experimental enthalpy of formation for propargyl cation, is in good agreement with the calculated $\Delta H_f^o{}_{298}$(propargyl radical) = 285.5 kcal/mol.

Because cycloprop-2-enyl anion is very unstable, its $\Delta H_f^o{}_{298}$ is not known from experiment. Previous theoretical studies using the G2 theory by Glukhovtsev et al.[29] indicated that $\Delta H_f^o{}_{298}$(cycloprop-2-enyl anion) is between 110 and 122.3 kcal/mol. The $\Delta H_f^o{}_{298}$(cycloprop-2-enyl anion) = 118.5 kcal/mol computed at the UCCSD(T)/6-311+G(3df,2p) level in combination with the isodesmic reaction 36 lies in the range predicted in ref 29.

On the basis of the heats formation for C_3H_3 radicals and their charged species, we can arrange their stabilities as follows: **1**• > **2**• > **3**• ≈ **4**•; **2**$^+$ > **1**$^+$ > **3**$^+$; and **3**$^-$ > **1**$^-$ > **4**$^-$ > **2**$^-$. After losing an electron, C_3H_3 radicals tend to close the ring to cycloprop-2-enyl anion (**2**$^+$), which is the most stable among cation species and has two π electrons in the cycle satisfying the aromatic rule of $4n + 2$ electrons ($n = 0$). However, adding an electron to the C_3H_3 radicals likely leads to the 1-propynyl anion (**3**$^-$).

4.3.2. Thermochemistry for C$_3$H$_4$. The C$_3$H$_4$ isomers (including propyne, allene, and cyclopropene) are neutral species with an even number of electrons and are very stable. Therefore,

they are easily characterized by experimental measurements and high-level theoretical calculations. While the enthalpies of formation for C$_3$H$_4$ isomers were computed using the G3 theory by Pople and co-workers,[49] the other thermochemical parameters such as IP, C−H BDE, and gas-phase acidity (GPA) are not available. These properties calculated at the G3 and UCCSD-(T) levels are presented in the Table 8. As seen in Table 8, the computed thermochemical values at the UCCSD(T) level are close to those obtained at the G3 theory and in good agreement with the experimental data. When the number of electron pairs is not conserved in the reactions (addition of e$^-$ or H), the thermochemical parameters calculated at the UCCSD(T) level using these reactions are worse than those from the G3 theory. In such cases, the CCSD(T)/B3LYP approach in combination with isodesmic reactions lead to the better results, which agree well with the G3 results and the experimental data. On the other, when the number of electron pairs is conserved (addition of H$^+$), the properties derived from such reactions are similar to those calculated from isodesmic reactions and in good agreement with experimental results.

4.3.3. Heats of Formation for C$_3$H$_2$ and C$_3$H Species. The enthalpy of formation for *c*-C$_3$H$_2$ is still controversial. The experimental $\Delta H_f^o{}_{298}(c\text{-}C_3H_2) = 114 \pm 4$ kcal/mol determined by Clauberg et al.[28] was derived from measured ionization energy for *c*-C$_3$H$_2$ (9.15 ± 0.03 eV)[28] and a literature value of 322 ± 4 kcal/mol for $\Delta H_f^o{}_{298}(c\text{-}C_3H_2^{\bullet+})$,[41] which was confirmed to be incorrect.[39] The other experimental studies[42] lead to $\Delta H_f^o{}_{298}(c\text{-}C_3H_2^{\bullet+}) = 329$ kcal/mol, which is consistent with the theoretical value of 331.5 kcal/mol recommended by Wong and Radom[43] using the G2 theory. Combining $\Delta H_f^o{}_{298}(c\text{-}C_3H_2^{\bullet+})$ = 329 kcal/mol[42] and IP(*c*-C$_3$H$_2$) = 9.15 ± 0.03 eV,[28] the new experimental value of 118.0 kcal/mol for *c*-C$_3$H$_2$ is obtained. This is in good agreement with the experimental $\Delta H_f^o{}_{298}(c\text{-}C_3H_2)$ = 119.5 ± 2.2 kcal/mol deduced by Chyall and Squires,[39] the theoretical values of 119.2 kcal/mol determined by Wong and Radom[43] employing the G2 theory, 118.9 kcal/mol calculated by Montgomery et al.[16] at the CBS-QCI/APNO level of theory, and 119.0 kcal/mol estimated by Vereecken et al.[5]
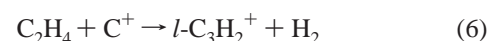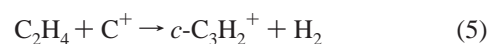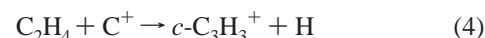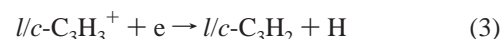
To reinvestigate $\Delta H_f^o{}_{298}(c\text{-}C_3H_2)$, we utilize the UCCSD(T)/6-311+G(3df,2p)//B3LYP/6-311G(d,p) level of theory in combination with the isodesmic reaction 53 (see Table 9). From the heat of reaction of 69.4 kcal/mol, $\Delta H_f^o{}_{298}(CH_4) = -17.9$ kcal/mol,[30] $\Delta H_f^o{}_{298}(c\text{-}C_3H_4) = 66.2$ kcal/mol,[44] and $\Delta H_f^o{}_{298}$[CH$_2$(^{1}A$_1$)] = 102.7 kcal/mol,[44] the value of 117.4 kcal/mol is derived for the heat of formation of *c*-C$_3$H$_2$. $\Delta H_f^o{}_{298}(c\text{-}C_3H_2)$ can be also determined from PA(*c*-C$_3$H$_2$) = 225.4 kcal/mol at the UCCSD(T) level, $\Delta H_f^o{}_{298}(H^+) = 365.7$ kcal/mol,[30] and $\Delta H_f^o{}_{298}(c\text{-}C_3H_3^+) = 257.3 \pm 0.8$ kcal/mol.[31] The value of 117.0 kcal/mol is obtained in this case. On the basis of the theoretical calculations by us and other authors[5,16,43] and the corresponding experimental data,[28,39,42] we suggest the new value of 118.0 ± 1 kcal/mol for the enthalpy of formation of singlet cylopropenylidene.

The calculated $\Delta H_f^o{}_{298}(H_2CCC)$ and $\Delta H_f^o{}_{298}$[HCCCH(^{1}A$_1$)] also lie about 4 kcal/mol higher than the experimental data determined by Clauberg et al.[28] (see reactions 54 and 56 in Table 9). $\Delta H_f^o{}_{298}$[HCCCH(^{3}B)], computed from the iosdesmic reaction 55, is 132.7 kcal/mol which agrees well with the theoretical $\Delta H_f^o{}_0$[HCCCH(^{3}B)] = 132.2 kcal/mol at the CCSD(T)/cc-pVQZ//CCSD(T)/TZP level of theory.[45] For C$_3$H species, the calculated $\Delta H_f^o{}_{298}$ from two different working reactions are consistent. Taking their average, the $\Delta H_f^o{}_{298}$[HCCC($^2\Pi$)] = 172.7 kcal/mol and $\Delta H_f^o{}_{298}(c\text{-}C_3H)$ = 169.8 kcal/mol can be proposed.

5. Astrophysical Implications

The singlet cyclopropenylidene isomer *c*-C$_3$H$_2$, was detected in 1985 via microwave spectroscopy in the interstellar medium.[66] Subsequent quantitative surveys indicated that *c*-C$_3$H$_2$ is one of the most abundant molecules in interstellar environments such as dark clouds TMC-1, Oph A, Ori A, and SgrB2 as well as the carbon star IRC +10216 with fractional abundances up to 10^{-8} cm^{-3}.[1] In diffuse clouds, cyclopropenylidene is depleted by a factor of about 100.[67] A second C$_3$H$_2$ isomer, singlet vinylidenecarbene (H$_2$CCC), was discovered 6 years later by Cernicharo et al. toward TMC-1.[68] Compared to cyclopropenylidene, its fractional abundance is only 1−2%. Most surprisingly however, a third isomer triplet propargylene− although more stable than vinylidenecarbene−has never been observed in the ISM.

Our theoretical investigation of the C$_3$H$_3$ PES together with possible C$_3$H$_2$ species classify the C(^{3}P)/C$_2$H$_3$ system as a possible keystone to form C$_3$H$_2$ isomers in extraterrestrial environments. Although detailed RRKM studies are still ongoing, this neutral−neutral reaction represents a strong alternative to hitherto postulated reaction sequence:

$$C_2H_2 + C^+ \rightarrow l/c\text{-}C_3H^+ + H \quad (1)$$

$$l/c\text{-}C_3H^+ + H_2 \rightarrow c\text{-}C_3H_3{}^+ + h\nu \quad (2)$$

$$l/c\text{-}C_3H_3{}^+ + e \rightarrow l/c\text{-}C_3H_2 + H \quad (3)$$

$$C_2H_4 + C^+ \rightarrow c\text{-}C_3H_3{}^+ + H \quad (4)$$

$$C_2H_4 + C^+ \rightarrow c\text{-}C_3H_2{}^+ + H_2 \quad (5)$$

$$C_2H_4 + C^+ \rightarrow l\text{-}C_3H_2{}^+ + H_2 \quad (6)$$

$$l/c\text{-}C_3H_3{}^+ + e \rightarrow l/c\text{-}C_3H_2 + H \quad (7)$$

This previous speculated reaction mechanism cannot account for fractional abundances, isomer ratios of *c*-C$_3$H$_2$ vs H$_2$CCC, or high deuterium enrichment observed in *c*-C$_3$HD vs *c*-C$_3$H$_2$, i.e. an observed value of 0.08 in TMC-1 vs 0.015 as obtained in chemical models. Hence, the reaction of atomic carbon with the vinyl radical can replace the ion−molecule based four- to five-step synthesis through a **single** reactive encounter to form C$_3$H$_2$ isomers. Preliminary crossed beam data on the C(^{3}P)/C$_2$H$_3$ reaction detected indeed the carbon vs hydrogen atom exchange to form C$_3$H$_2$ as monitored at m/e = 38 via C$_3$H$_3$ complex(es). But further experimental studies combines with isotopically labeled C$_2$H$_3$ are necessary to unravel the reaction products experimentally.

6. Conclusions

(a) The C(^{3}P) + C$_2$H$_3$ reaction produces vibrationally excited C$_3$H$_3$ intermediates **4** and **5** on the ground-state PES without barrier, which have enough energy to interconvert to the other C$_3$H$_3$ isomers, **1**−**3**. H$_2$ or H eliminations then lead to the C$_3$H or C$_3$H$_2$ fragments, respectively. The most energetically favorable pathway is the formation of *c*-C$_3$H$_2$ by splitting H from **2**. Hence, the C(^{3}P) + C$_2$H$_3$ reaction could form *c*-C$_3$H$_2$ via a multistep mechanism involving C$_3$H$_3$ intermediates. However, the other reaction mechanisms leading to H$_2$CCC + H, HCCCH-(^{3}B) + H, and H$_2$ + HCCC exhibit barriers only 1−5 kcal/mol higher than those to produce H + *c*-C$_3$H$_2$. Therefore, detailed

RRKM calculations are required to predict the product branching ratios under various reaction conditions.

(b) The $C(^3P) + C_2H_3$ entrance channel yields isomers **4es** and **5es** on the first excited doublet state PES, which then interconvert to **1es**. The C−H bond fission of **1es** leads to **P1es** (HCCCH, $1^1A''$). This product channel on the excited-state PES is much more favorable than the production of excited H_2CCC-(1^1A_2) or c-$C_3H_2(1^1A_2$). In a denser environment $HCCCH(1^1A'')$ can react with atomic hydrogen rapidly producing $HCCC(1^2\Pi)$ + H_2 virtually without barrier.

(c) Summarizing, we can give following $\Delta H_f^o{}_{298}(C_3H_n)$ values as our recommendation: $\Delta H_f^o{}_{298}(H_2CCCH) = 84.5 \pm 1$ kcal/mol, $\Delta H_f^o{}_{298}(c$-$C_3H_3) = 114.5 \pm 2$ kcal/mol, $\Delta H_f^o{}_{298}(H_3CCC) = 124 \pm 2$ kcal/mol, $\Delta H_f^o{}_{298}(c$-$C_3H_2) = 118.0 \pm 1$ kcal/mol, $\Delta H_f^o{}_{298}(H_2CCC) = 133 \pm 1$ kcal/mol, $\Delta H_f^o{}_{298}[HCCCH(^3B)] = 132.5 \pm 1$ kcal/mol, $\Delta H_f^o{}_{298}[HCCCH(^1A_1)] = 144 \pm 1$ kcal/mol, $\Delta H_f^o{}_{298}[HCCC(^2\Pi)] = 173 \pm 2$ kcal/mol, and $\Delta H_f^o{}_{298}(c$-$C_3H) = 170 \pm 2$ kcal/mol. The use of the UCCSD(T)/6-311+G(3df,2p)//B3LYP/6-311G(d,p) + TC[B3LYP/6-311G(d,p)] approach scheme in combination with isodesmic reactions leads to the results, which are well-consistent with the available experimental data. The differences between our best theoretical results and experimental data do not exceed 1−2 kcal/mol, which lies within experimental error bars.

(d) In general, thermochemical properties calculated at the G3 theory are close to those at the UCCSD(T)/6-311+G-(3df,2p)//B3LYP/6-311G(d,p) level of theory and agree well with experiment. However, when a species has high spin-contamination, G3 results may not be as accurate.

References and Notes

(1) (a) Green, S. *Astrophys. J.* **1980**, *240*, 962. (b) Turner, B. E. *Astrophys. J. Lett.* **1989**, *347*, L39. (c) Thaddeus, P.; Vrtilek, J. M.; Gottlieb, C. A. *Astrophys. J. Lett.* **1985**, *299*, 63. (d) Kuiper, T. B.; Whiteoak, J. B.; Peng, R. S.; Peter III, W. L.; Reynolds, J. E. *Astrophys. J. Lett.* **1993**, *416*, 33.

(2) Kaiser, R. I.; Ochsenfeld, C.; Stranges, D.; Head-Gordon, M.; Lee, Y. T. *Faraday Discuss.* **1998**, *109*, 183.

(3) Madden, S. C. In *Chemistry in Space*; Greenberg, J. M., Pirronello, V., Eds.; Kluwer: Dordrecht, 1991; p 437 and references therein.

(4) (a) Walch, S. P. *J. Chem. Phys.* **1995**, *103*, 7064. (b) Guadagnini, R.; Schatz, G. C.; Walch, S. P. *J. Phys. Chem. A* **1998**, *102*, 5857.

(5) Vereecken, L.; Pierloot, K.; Peeters, J. *J. Chem. Phys.* **1998**, *108*, 1068.

(6) Mebel, A. M.; Jackson, W. M.; Chang, A. H. H.; Lin, S. H. *J. Am. Chem. Soc.* **1998**, *120*, 5751.

(7) Deyerl, H. J.; Fischer, I.; Chen, P. *J. Chem. Phys.* **1999**, *111*, 3441.

(8) Jackson, W. M.; Anex, D. S.; Continetti, R. E.; Balko, B. A.; Lee, Y. T. *J. Chem. Phys.* **1991**, *95*, 7327.

(9) Wu, C.; Kern, R. J. *Chem. Phys.* **1987**, *91*, 6291.

(10) (a) Alkemade, V.; Homann, K. Z. *Phys. Chem. Neue Folge* **1989**, *161*, 19. (b) Kern, R. D.; Singh, H. J.; Wu, C. H. *Int. J. Chem. Kinet.* **1988**, *20*, 731. (c) Westmoreland, P.; Dean, A.; Howard, J.; Longwell, J. *J. Chem. Phys.* **1989**, *93*, 8171. (d) Hidaka, Y.; Nakamura, T.; Miyauchi, A.; Shiraishi, T.; Kawano, H. *Int. J. Chem. Kinet.* **1989**, *29*, 643. (e) Stein, S.; Walker, J.; Suryan, M.; Farh, A. *23rd Symp. (Int.) Comb.* **1991**, 85. (f) Miller, J.; Melius, C. *Combust. Flame* **1992**, *91*, 21. (g) Melius, C. F.; Miller, J. A.; Evleth, E. M. *24th Symp. (Int.) Comb.* **1993**, 621. (h) Morter, C.; Farhat, S.; Adamson, J.; Glass, G.; Curl, R. *J. Phys. Chem.* **1994**, *98*, 7029. (i) Kern, R. D.; Chen, H.; Kiefer, J. H.; Mudipalli, P. S. *Combust. Flame* **1995**, *100*, 177. (j) Miller, J. A.; Volponi, J. V.; Pauwels, J.-F. *Combust. Flame* **1996**, *105*, 451.

(11) Botschwina, P.; Oswald, R.; Flugge, J.; Horn, M. *Z. Phys. Chem.* **1995**, *188*, 29.

(12) (a) Minsek, D. W.; Chen, P. *J. Phys. Chem.* **1990**, *94*, 8399. (b) Lossing, F. P. *Can. J. Chem.* **1972**, *50*, 3973. (c) Jacox, M. E.; Milligan, D. E. *Chem. Phys.* **1974**, *4*, 45. (d) Huang, J. W.; Graham, W. R. *J. Chem. Phys.* **1990**, *93*, 1583. (e) Tanaka, K.; Harada, T.; Sumiyoshi, Y.; Tanaka, T. 22nd International Symposium on Free Radicals, Doorwerth, The Netherlands, Sept 6−10, 1993; Abstr. B-22.

(13) Honjou, H.; Yoshimime, M.; Pacansky, J. *J. Phys. Chem.* **1987**, *91*, 4455.

(14) Farh, A.; Hassanzadeh, P.; laszlo, B.; Huie, R. E. *Chem. Phys.* **1997**, *215*, 59.

(15) Gillbert, T.; Pfab, R.; Fischer, I.; Chen, P. *J. Chem. Phys.* **2000**, *112*, 2575.

(16) Montgomery, J. A., Jr.; Ochterski, J. W.; Petersson, G. A. *J. Chem. Phys.* **1994**, *101*, 5900.

(17) Song, X.; Bao, Y.; Urdahl, R. S.; Grosine, J. N.; Jackson, W. M. *Chem. Phys. Lett.* **1994**, *217*, 216.

(18) Jackson, W. M. In *Comets in the Post-Halley Era*; Newburn, R. L., Ed.; Kluwer Academic Publishers: Amsterdam, 1991; Vol. 1, p 313.

(19) (a) Seki, K.; Okabe, H. *J. Phys. Chem.* **1992**, *96*, 3345. (b) Satyapal, S.; Bersohm, R. *J. Phys. Chem.* **1991**, *95*, 8004. (c) Sun, W.; Yokoyama, K.; Robinson, J. C.; Suits, A. G.; Neumark, D. M. *J. Chem. Phys.* **1999**, *110*, 4263. (d) Ni, C. K.; Huang, J. D.; Chen, Y. T.; Kung, A. H.; Jackson, W. M. *J. Chem. Phys.* **1999**, *110*, 3320.

(20) Stanton, J. F. *Chem. Phys. Lett.* **1995**, *237*, 20.

(21) Yamanoto, S.; Saito, S. *J. Chem. Phys.* **1994**, *101*, 5484.

(22) Takahashi, J.; Yamashita, K. *J. Chem. Phys.* **1996**, *104*, 6613.

(23) Melius, C. F. *BAC-MP4 Heats of Formation and Free Energies*; Sandia National Laboratories: Livermore, CA, 1996.

(24) Robinson, M. S.; Polak, M. L.; Bierbaum, V. M.; Depuy, C. H.; Lineberger, W. C. *J. Am. Chem. Soc.* **1995**, *117*, 6766.

(25) Roth, W. R.; Hoff, H.; Horn, C. *Chem. Ber.* **1994**, *127*, 1781.

(26) Defrees, D. J.; McIver, R. T.; Hehre, W. J. *J. Am. Chem. Soc.* **1980**, *102*, 3335.

(27) An ESR study (Closs, G. L.; Redwine, O. D. *J. Am. Chem. Soc.* **1986**, *108*, 506) and ab initio studies (Chipman, D. M.; Miller, K. E. *J. Am. Chem. Soc.* **1984**, *106*, 6236; Byun, Y. G.; Saebo, S.; Pittman, C. U. *J. Am. Chem. Soc.* **1991**, *113*, 3689).

(28) Clauberg, H.; Minsek, D. W.; Chen, P. *J. Am. Chem. Soc.* **1992**, *114*, 99.

(29) Glukhovtsev M. N.; Laiter, S.; Pross, A. *J. Phys. Chem.* **1996**, *100*, 17801.

(30) NIST Chemistry WebBook, http://webbook.nist.gov/chemistry/, NIST Standard Reference Database Number 69, February 2000 release.

(31) Lias, S. G.; Bartmess, J. E.; Liebman, J. F.; Holmes, J. L.; Levin, R. D.; Mallard, W. G. *J. Phys. Chem. Ref. Data* **1988**, *17* (Suppl. 1).

(32) Oakes, J. M.; Ellison, G. B. *J. Am. Chem. Soc.* **1983**, *105*, 2969.

(33) Ikuta, S. *J. Mol. Struct.* (*THEOCHEM*) **1998**, *434*, 121.

(34) Bartmess. J. E.; Scott, J. A.; McIver, R. T., Jr. *J. Am. Chem. Soc.* **1979**, *101*, 6046.

(35) Li, W. K.; Riggs, N. V. *J. Mol. Struct.* (*THEOCHEM*) **1992**, *257*, 189.

(36) King, K. D.; Nguyen, T. T. *J. Phys. Chem.* **1979**, *83*, 1940.

(37) Tsang, W. *Int. J. Chem. Kinet.* **1970**, *2*, 23.

(38) Yang, Z. Z.; Wang, L. S.; Lee, Y. T.; Shirley, D. A.; Huang, S. Y.; Lester, W. A, Jr. *Chem. Phys. Lett.* **1990**, *171*, 9.

(39) Chyall, L. J.; Squires, R. R. *Int. J. Mass Spectrom. Ion Processes* **1995**, *149/150*, 267.

(40) Reisenaur, H. P.; Maier, G.; Riemann, A.; Hoffmann, R. W. *Angew. Chem.* **1984**, *96*, 596; *Angew. Chem., Int. Ed. Engl.* **1984**, *23*, 641.

(41) Prodnuk, S. D.; Depuy, C. H.; Bierbaum, V. M. *Int. J. Mass Spectrom. Ion Processes* **1990**, *100*, 693.

(42) (a) Dannacher, J.; Heilbronner, E.; Stadelamn, J.; Vogt, J. *Helv. Chim. Acta* **1979**, *62*, 2186. (b) Smith, D.; Adams, N. G. *Int. J. Mass Spectrom. Ion Processes* **1987**, *76*, 307. (c) Smith, D.; Adams, N. G.; Ferguson, E. E. *Int. J. Mass Spectrom. Ion Processes* **1984**, *61*, 15.

(43) Wong, M. W.; Radom, L. *J. Am. Chem. Soc.* **1993**, *115*, 1507.

(44) Pedley, J. B.; Naylor, R. D.; Kirby, S. P. *Thermochemical Data for Organic Compounds*, 2nd ed.; Chapman and Hall: London, 1996.

(45) (a) Ochsenfeld, C.; Kaiser, R. I.; Lee, Y. T.; Suits, A. G.; Head-Gordon, M. *J. Chem. Phys.* **1997**, *106*, 4141. (b) Kaiser, R. I.; Ochsenfeld, C.; Head-Gordon, M.; Lee, Y. T.; Suits, A. G. *J. Chem. Phys.* **1997**, *106*, 1729.

(46) Ikuta, S. *J. Chem. Phys.* **1997**, *106*, 4541.

(47) (a) Purvis, G. D.; Bartlett, R. J. *J. Chem. Phys.* **1982**, *76*, 1910. (b) Hampel, C.; Peterson, K. A.; Werner, H.-J. *Chem. Phys. Lett.* **1992**, *190*, 1. (c) Knowles, P. J.; Hampel, C.; Werner, H.-J. *J. Chem. Phys.* **1994**, *99*, 5219. (d) Deegan, M. J. O.; Knowles, P. J. *Chem. Phys. Lett.* **1994**, *227*, 321.

(48) MOLPRO is a package of ab initio programs written by: Werner, H.-J.; Knowles, P. J. with contributions from Almlöf, J.; Amos, R. D.; Deegan, M. J. O.; Elbert, S. T.; Hampel, C.; Meyer, W.; Peterson, K.; Pitzer, R.; Stone, A. J.; Taylor, P. R.; Lindh, R.

(49) Curtiss, L. A.; Raghavachari, K.; Redfern, P. C.; Rassolov, V.; Pople J. A. *J. Chem. Phys.* **1998**, *109*, 7764.

(50) (a) Becke, A. D. *J. Chem. Phys.* **1993**, *98*, 5648. (b) Becke, A. D. *J. Chem. Phys.* **1992**, *96*, 2155. (c) Becke, A. D. *J. Chem. Phys.* **1992**, *97*, 9173. (d) Lee, C., Yang, W.; Parr, R. G. *Phys. Rev.* **1988**, *B37*, 785.

(51) (a) Pople, J. A.; Head-Gordon, M.; Raghavachari, K. *J. Chem. Phys.* **1987**, *87*, 5968. (b) Gauss, J.; Cremer, C. *Chem. Phys. Lett.* **1988**, *150*, 280. (c) Trucks, G. W.; Frisch, M. J. *Semi-Direct QCI Gradients* **1998**. (d) Salter, E. A.; Trucks, G. W.; Barlett, R. J. *J. Chem. Phys.* **1989**, *90*, 1752. (e) Lee, T. J.; Taylor, P. R. *Int. J. Quantum Chem. Symp.* **1989**, *23*, 199. (f) Lee, T. J.; Rendell, A. P.; Taylor, P. R. *J. Phys. Chem.* **1990**, *94*, 5463.

(52) (a) Purvis, G. D.; Bartlett, R. J. *J. Chem. Phys.* **1982**, *76*, 1910. (b) Scuseria, G. E.; Janssen, C. L.; Schaefer III, H. F. *J. Chem. Phys.* **1988**, *89*, 7382. (c) Scuseria, G. E.; Schaefer III, H. F. *J. Chem. Phys.* **1989**, *90*, 3700. (d) Pople, J. A.; Head-Gordon, M.; Raghavachari, K. *J. Chem. Phys.* **1987**, *87*, 5968.

(53) (a) Bauschlicher, C. W., Jr.; Partridge, H. *J. Chem. Phys.* **1995**, *103*, 1788. (b) Bauschlicher, C. W., Jr.; Partridge, H. *Chem. Phys. Lett.* **1995**, *240*, 533.

(54) (a) Mebel, A. M.; Morokuma, K.; Lin, M. C. *J. Chem. Phys.* **1995**, *103*, 7414. (b) Mebel, A. M.; Morokuma, K.; Lin, M. C.; Melius, C. F. *J. Phys. Chem.* **1995**, *99*, 1900. (c) Mebel, A. M.; Morokuma, K.; Lin, M. C. *J. Chem. Phys.* **1995**, *103*, 3440.

(55) (a) Werner, H.-J.; Knowles, P. J. *J. Chem. Phys.* **1985**, *82*, 5053. (b) Knowles, P. J.; H.-J. *Chem. Phys. Lett.* **1985**, *115*, 259.

(56) (a) Werner, H.-J.; Knowles, P. J. *J. Chem. Phys.* **1988**, *89*, 5803. (b) Knowles, P.-J.; Werner, H.-J. *Chem. Phys. Lett.* **1988**, *145*, 514.

(57) Widmark, P.-O.; Malmqvist, P.-A.; Roos, B. O. *Theoret. Chim. Acta* **1990**, *77*, 291.

(58) Serrano-Andres, L.; Merchan, M.; Nebot-Gil, I.; Lindh, R.; Roos, B. O. *J. Chem. Phys.* **1993**, *98*, 3151.

(59) Curtiss, L. A.; Raghavachari. K.; Trucks, G. W.; Pople, J. A. *J. Chem. Phys.* **1991**, *94*, 7221.

(60) (a) Mayer, P. M.; Parkinson, C. J.; Smith, D. M.; Radom, L. *J. Chem. Phys.* **1998**, *108*, 604. (b) Parkinson, C. J.; Mayer, P. M.; Radom, L. *J. Chem. Soc., Perkin Trans. 2* **1999**, 2305.

(61) (a) Curtiss, L. A.; Raghavachari. K.; Redfern, P. C.; Pople, J. A. *J. Chem. Phys.* **1997**, *106*, 1063; *J. Chem. Phys.* **1998**, *109*, 42; *J. Chem. Phys.* **2000**, *112*, 7374. (b) Montgomery, J. A., Jr.; Frisch, M. J.; Ochterski, J. W.; Petersson, G. A. *J. Chem. Phys.* **1999**, *110*, 2822.

(62) Frisch, M. J.; Trucks, G. W.; Schlegel, H. B.; Scuseria, G. E.; Robb, M. A.; Cheeseman, J. R.; Zakrzewski, V. G.; Montgomery, J. A. Jr.; Stratmann, R. E.; Burant, J. C.; Dapprich, S.; Millam, J. M.; Daniels, A. D.; Kudin, K. N.; Strain, M. C.; Farkas, O.; Tomasi, J.; Barone, V.; Cossi, M.; Cammi, R.; Mennucci, B.; Pomelli, C.; Adamo, C.; Clifford, S.; Ochterski, J.; Petersson, G. A.; Ayala, P. Y.; Cui, Q.; Morokuma, K.; Malick, D. K.; Rabuck, A. D.; Raghavachari, K.; Foresman, J. B.; Cioslowski, J.; Ortiz, J. V.; Stefanov, B. B.; Liu, G.; Liashenko, A.; Piskorz, P.; Komaromi, I.; Gomperts, R.; Martin, R. L.; Fox, D. J.; Keith, T.; Al-Laham, M. A.; Peng, C. Y.; Nanayakkara, A.; Gonzalez, C.; Challacombe, M.; Gill, P. M. W.; Johnson, B.; Chen, W.; Wong, M. W.; Andres, J. L.; Gonzalez, C.; Head-Gordon, M.; Replogle, E. S.; Pople, J. A. *GAUSSIAN 98*, revision A.5; Gaussian Inc.: Pittsburgh, PA, 1998.

(63) Scott, A. P.; Radom, L. *J. Phys. Chem.* **1996**, *100*, 16502.

(64) Sharma, D. K. S.; Franklin, J. L. *J. Am. Chem. Soc.* **1973**, *95*, 6562.

(65) Bauschlicher, Jr., C. W.; Langhoff, S. R. *Chem. Phys. Lett.* **1992**, *193*, 380.

(66) (a) Thaddeus P.; Vrtilek, J. M.; Gottlieb, C. A. *Astrophys. J. Lett.* **1985**, *299*, 63. (b) Matthews, H. E.; Irvine, W. M. *Astrophys. J. Lett.* **1985**, *298*, 61.

(67) Turner, B. E.; Rickard, L. J.; Xu, L. P. *Astrophys. J.* **1989**, *344*, 292.

(68) Cernicharo, J.; et al. *Astrophys. J. Lett.* **1991**, *368*, 39.